universität wien

DIPLOMARBEIT

Titel der Diplomarbeit

„Inherent characteristics of the dsDNA binding dyes EvaGreen®, Sybr® Green and SYTO® 9 in multiplexed PCR setups“

Band 1 von 1

Verfasser

Georg Mair

angestrebter akademischer Grad

Magister der Naturwissenschaften (Mag.rer.nat.)

Wien, September 2013

Studienkennzahl lt. Studienblatt:	A 441
Studienrichtung lt. Studienblatt:	Mikrobiologie und Genetik
Betreuerin / Betreuer:	Ao.Univ.-Prof. Dr.rer.nat. Ralf Steinborn

VetCore, Genomics Core Facility,
University of Veterinary Medicine Vienna
(Ao.Univ.-Prof. Dr.rer.nat. Ralf Steinborn)

Inherent characteristics of the dsDNA binding dyes EvaGreen®, Sybr® Green and SYTO® 9 in multiplexed PCR setups

Diploma Thesis
in order to obtain a Degree of
MAGISTER RERUM NATURALIUM
of the University of Vienna

---

submitted by:
Georg Mair

“They all try and figure out why I’m different.”

(by Eva Green, in Marie Claire Magazine)

Acknowledgements

First and foremost I would like to express my gratitude to Ao.Univ.-Prof. Dr.rer.nat. Ralf Steinborn for providing me the opportunity to make my diploma thesis at his facility and the kindly reviewing of this work.. He spent a lot of time for guidance and support, patience for discussions and helpful advice and remarks on my work.

Special thanks go to Dr.med.vet. Hermann Unger, of the Department of Nuclear Sciences and Applications, International Atomic Energy Agency (IAEA) Vienna, for his support and wise remarks. He always offered time to discuss and refresh the content of my thesis and really pushed me for the benefit of finishing this work.

I would like to thank Ao.Univ.-Prof. Dr.med.vet. Dieter Klein for the opportunity to work at VetCore Facility for Research at the University of Veterinary Medicine Vienna.

I would like to thank Mag.rer.nat. Sonja Sabitzer, Mag.rer.nat Katharina Nöbauer, Msc. Stefanie Burger and Dr.rer.nat. Karin Hummel of VetCore for their help and being a group of wonderful colleagues during my work.

Many thanks to O.Univ.-Prof. Dr.med.vet. Gottfried Brem, Institute of Animal Breeding and Genetics/IFA Tulln Biotechnology, and Dr.rer.nat Gerald Hochwimmer for providing the samples for the experiments. Without this material this work would not have been possible.

A special thank goes to Dr. Stephan Winkler, FH Hagenberg, for the cooperation and his mathematical technical support as well as his support as a good friend.

I would like to give my special thanks to my parents for their support and love through all this long process. Thank you more than thousand times Mum and Dad!

Special thanks also to my mother, father and sister in law with her small and lovely family for their support. Wolfgang, I will never forget you and miss the lively discussions!

Finally I want to express my deepest gratitude to my wife, best friend and love Kerstin for being my sunshine, laughter and halt.

Contents

LIST OF ABBREVATIONS

A	adenine
A/T	adenine or thymidine
AT	adenine and thymidine
ARMS	amplification refractory mutation system
BLAST	Basic Local Alignement Tool
bp	basepair
C	cytosine
cDNA	complementary DNA
Cq	cycle of quantification (quantification cycle)
-dF / dT	negative derivative fluorescence per derivative temperature
DMSO	dimethyl solfoxide
DNA	deoxyribonucleic acid
dNTP	deoxyribonucleoside 5’ triphosphate
dsDNA	double stranded deoxyribonucleic acid
E	amplification efficiency
EDTA	ethylenediaminetetraacetic acid
EG	EVAGreen
EtBr	ethidium bromide
FAM	reporter dye 6-carboxyfluorescein
G	guanine
G / C	guanidine or cytosine
GC	guanidine and cytosine
grd	degree
HCL	hydrochloric acid
HRM	high resolution melting
kb	kilo bases
LCGreen	LightCycler Green
max	maximum
MCA	melting curve analysis
Mg^{++}	magnesium ion
$MgCl_2$	magnesium chloride
miRNA	microRNA

min	minute
µl	microliter
mM	millimolar
NCBI	National Center for Biotechnology Information
ng	nanogram
nm	nanometer
nM	nanomolar
NMR	nuclear magnetic resonance analysis
NN	nearest neighbour algorithm
nt	nucleotides
NTC	no template control
OD	optical density
pg	picogram
pH	power of hydrogen
PCR	polymerase chain reaction
pmol	picomol
PrP	prion protein
QA	quality assurance
qPCR	quantitative real-time PCR
RCA	re-association curve analysis
RNA	ribonucleic acid
S9	SYTO9
SB	sodium borate
s	second
SG	Sybr® Green
SNP	single nucleotide polymorphism
ss	single stranded
SSB	single stranded binding protein
ssDNA	single stranded DNA
T / °C	temperature in degree celcius
T	thymidine
TAE	Tris-acetate and EDTA buffer
Taq	DNA polymerase of *Thermus aquaticus*
TE	Tris and EDTA buffer

Tm	melting temperature
Tris	tris(hydroxymethyl)aminomethane
U	unit
w/v	weight per volume
-x	-times
3’	three prime
5’	five prime
ΔCq	difference in quantification cycle
ΔG	change in enthropy
ΔGC%	difference in guanine and cytosine percentage
ΔH	change in enthalpy
ΔT	difference in temperature
ΔTm	difference in melting temperature
%GC	guanosine and cytosine percentage

IV Summary

IV.1 Summary

Background

Intercalating dyes are commonly used for qPCR setups. If bound to double-stranded targets, they allow real time monitoring of amplification and closed-tube revision of targeted and co-amplified products by Melting Curve Analysis (MCA). In case of a homogenous dye distribution, the method allows multiplexing of two or more targets with different Tms. Contrary to the gold standard dye SybrGreen (SG), for which a GC content directed binding preference is assumed, such effects are not scrutinised for the more recently developed 3rd generation and HRM capable dye EvaGreen (EG) or other equivalent dyes. Therefore this study aimed at elaborating the performance of the dyes EG, SG and SYTO9 regarding the potential to saturate two targets, binding preference to nucleotides and the binding frequency to a sequence. Additionally hybridisation protocols were performed to characterise the different kinetics of the dyes interacting with dissociating and re-associating amplicons.

Methods

An in-house multiplex qPCR-MCA assay was used in addition to a single reaction genotyping approach and an assay to amplify a severely structured GC-rich amplicon to investigate the performance of EG and SG. The potential of saturation and sequence dependent binding patterns were traced with setups of defined template copy numbers. The comparison of amplicon melting and hybridisation was done with various sequences of different GC content and two sequences for which two melting domains were predicted with the heat map prediction tool POLAND.

Results and Discussion

Parallel detection of two targets multiplexed in one reaction was possible with EG contrary to SG. In case of an amplicon with high GC content SG even caused inhibition of the PCR or false genotyping results. Employing setups of defined template copy numbers with different GC content, however, identified that the recommended concentration of SG but not the recommended concentration of the HRM compatible dyes EG or SYTO9 was sufficient to saturate two targets. Regarding the binding preferences, it was shown that SG preferred GC-rich sequences contrary to SYTO9, while such an attribute was avoided for EG. A preferred interaction type was identified as intercalation for SG or assumed for S9 and related to their binding preference. Such distinct kinetics were not identified for the homogenously performing EG. Reduced fluorescence maxima of the GC-rich amplicon peaks were due to quenching effects caused by the dimeric structure of this dye and the sequence moieties. Dye molecule relocation was only possible with S9. The comparison of the melting and hybridisation protocols identified a higher concurence of the latter regarding the thermodynamics of the dye / sequence interaction as the predicted melting temperatures (Tm) only matched the temperature values in re-associating amplicons.

IV.2 Zusammenfassung

Hintergrund

Interkalierende Farbstoffe werden routinemäßig zur "Echtzeit"-Darstellung der Sequenzamplifikation (z.B. basierend auf der PCR) verwendet. Aufgrund der Tatsache, dass diese Moleküle mit allen doppelsträngigen Nukleotidketten interagieren können, ermöglichen sie zusätzlich den Nachweis der spezifisch und unspezifisch amplifizierten Produkte mittels der Definition von Temperaturcharakteristika durch eine Schmelzkurven-Analyse. Dadurch können mit berechneten Temperaturunterschieden verschiedene Produkte differenziert werden. Dies jedoch nur unter der Voraussetzung, dass eine homogene Verteilung der Farbstoffmoleküle erfolgte. Dieser Voraussetzung stehen unter anderem sequenz- oder nukleotid-spezifische Bindungspräferenzen der Farbstoffe entgegen, kontraproduktive Attribute, die für den qPCR-Standardfarbstoff SG mehrfach beschrieben wurden. Für die neuen Moleküle der 3ten und HRM-fähigen Generation stehen derartige Informationen wie im Fall von EG nur rudimentär zur Verfügung. Das Ziel dieser Arbeit war daher, die Leistungsfähigkeit der Farbstoffe EG, SG und SYTO9 für den Nachweis von verschiedenen Zielsequenzen mit MCA zu überprüfen. Dafür wurden vorrangig das Saturierungspotenzial, Bindungspräferenzen sowie die Zahl der von einer Sequenz gebundenen Farbstoffmoleküle untersucht. Ein zusätzlicher Versuchsansatz hob schließlich die unterschiedliche Interaktions-Kinetik der ausgewählten Farbstoffe mit dissoziierenden und re-assoziierenden DNA-Sequenzen hervor.

Methoden

Die Leistungsfähigkeit der Farbstoffe EG und SG wurde in erster Instanz mit einem im Labor etablierten qPCR-MCA Multiplex-Ansatz, einem speziellen Genotypisierungs- und einem Ansatz zum Nachweis eines GC-reichen und sekundärstruktur-bildenden Amplifikats untersucht. Die weiteren Fragestellungen, wie das Saturierungspotenzial oder Bindungspräferenzen wurden mit einer Vielzahl von Produkten getestet. Die Dissoziation und Hybridisierung wurde mit zwei Sequenzen, die laut POLAND-Software energetisch unterschiedliche Bereiche aufwiesen, sowie mit Sequenzen unterschiedlichen GC Gehalts verglichen

Ergebnisse und Diskussion

Die Multiplex-Analyse mittels qPCR-MCA war nur möglich mit EG, nicht aber mit SG. Als wahrscheinliche Erklärung dieses Versagens zeigte sich nicht die übliche Konzentration, sondern die hohe GC-Affinität von SG. Diese Präferenz verstärkt unter anderem die thermische Stabilität von möglichen Sekundärstrukturen und schränkte die Amplifikation einer GC-reichen Zielsequenz (*Pou3f1*) sowie die Reproduzierbarkeit bi-allelischer SNP-Genotypisierung mit SG massiv ein. EG konnte als einzigem Farbstoff kein basen-spezifisches Bindungverhalten nachgewiesen werden. Gefundene Unterschiede wurden auf die unterschiedlichen Elektronenwolken von AT- und GC-reichen Sequenzen zurückgeführt. Dieser moderatere Einfluss ermöglichte damit Multiplex-Analysen im Gegensatz zu SG.

Im Zuge dieser Experimente zeigte sich weiters, daß die gemessenen Schmelztemperaturen unterschiedlicher DNA-Sequenzen von berechneten Tm-Werten abwichen ($\Delta Tm > 2.5$ °C). Dies konnte den Einflüssen von Reaktionskomponenten zugeordnet werden, die die Dissoziation der Stränge verzögern und nicht wie $MgCl_2$ in Berechnungen eingebunden sind. Die Messung der Fluoreszenzänderung während der Reassoziierung von Einzelsträngen ermöglicht dagegen eine zeitlich bessere Abfolge, da die Komponenten erst nach dem Zusammenschluss binden können. Die mit dieser alternativen Analyse gemessenen unterschieden sich kaum von den berechneten Tm-Werten ($\Delta Tm < 0.6$ °C).

1 Introduction

1.1 Analysis of double stranded DNA sequences by Melting Curve Analysis

The quantitative increase of double-stranded DNA (dsDNA) sequences during quantitative real-time PCR (qPCR) can be monitored by sequence specific hydrolysis or hybridisation probes. An alternative detection format bases on sequence unspecific double stranded DNA binding dyes (dyes), such as Sybr Green (SG) or EvaGreen (EG) (Ponchel et al., 2003; Mao et al., 2007). Dye molecules typically bind any dsDNA, resulting in emitting high levels of fluorescence after this interaction (Zipper et al., 2004). While the amplification curve displayed with sequence specific formats is representative for only the target sequence (amplicon), curves determined with dsDNA binding dyes display signals of all amplicons and hence double stranded products (e.g. primer dimers or unspecific products). This effect requires to perform a quality control *post* amplification to reveal unspecific products and to determine false positive results (Eischeid, 2011). Specifically for dye-based qPCR the controlled thermal dissociation of the amplification products (amplicons), termed MCA, is an example of this type. Continually ramping the reaction temperature forces the double strands to dissociate at a specific temperature and thereby releases the dye molecules (Picard et al., 2006; Smith et al., 2009). The resulting decrease in fluorescence is measured against temperature increase and is depicted as the raw data plot of amplicon melting (Picard et al., 2006; Pryor and Wittwer, 2006; Rasmussen et al., 2007). The typically reported melting point is the inflexion point of the first derivative of the raw curve and is highly specific for a given amplicon (Elenitoba-Johnson et al., 2001; Rasmussen et al., 2007 and Figure 1). The first derivative of this raw plot is mostly displayed to allow an assay interpretation. The inflexion point of this curve marks the typically reported melting point (Tm), which is highly specific for a given amplicon (Elenitoba-Johnson et al., 2001; Rasmussen et al., 2007 and Figure 1).

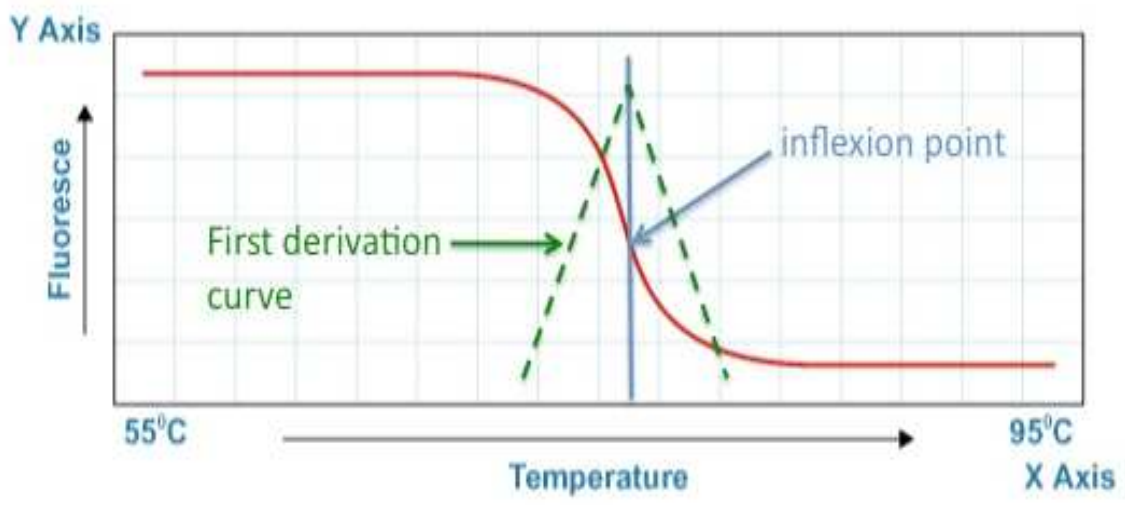

Figure 1: The "raw" melting profile is used to calculate the melting curves of MCA.
The first derivative depicts the commonly published melting curve, the climax of this curve marks the Tm, which is as well the inflexion point of the raw plot and the point at which half of the amplicons are already melted. This point is typically used as reference for quality control.

Today, MCA is used as an advanced quality control to discriminate for example several specific sequences in a multiplexed PCR setup (Ririe et al., 1997; Elenitoba-Johnson et al., 2001). This benefit is only assumed as the robustness of MCA is questionable chiefly because of scarce information on dye characteristics. The possibility to display different peaks in a multiplexed reaction for example relies on the fact that the dye molecules are spread in a homogenous way over the sequence (Hannah & Armitage, 2004). In the case of an uneven distribution, one amplicon specific peak might be lost (Giglio et al., 2003; Monis et al., 2005). Actually, it was demonstrated that directed binding of dyes or relocation of released dye molecules as a cause of such bias (Wittwer et al., Wipo Patent Publication WO/2004/038038, 2004). Such effects and other questions such as the definition of the number of dye molecules potentially interacting with a double strand, however, are so far not adressed. As the new generation dye EG in contrast is announced to be void of such effects and no experimental prove was published so far, this work addressed this issue (Mao et al, 2007; Eischeid, 2011; Meistertzheim et al., 2012).

1.1.1 Characteristics of dsDNA interacting dyes

The diversity of dyes useful to stain dsDNA is constantly increasing and each displays its very individual characteristic. The "first starters" such as the intercalating dye Ethidium Bromide

(Monaco, 2010) are still used for the issued protocols, although their biological safety is highly questionable (Singer et al., 1999 ; Monis et al., 2005). New generation or high saturation dyes such as SYTO® 9 (S9), LightCycler Green (LC green), BOXTO or EG allow saturation of a sequence with dye molecules without the inhibitory effects to the PCR reaction reported earlier (Eischeid, 2011). Due of that, reliable identification of SNP residues can be performed by an improved MCA approach termed high resolution melting (HRM) (Wittwer et al., 2003; Liew et al., 2004). Since the launch of Sybr® Green (SG) universal dye based protocols were developed and standardised (Singer et al., 1999; Varga and James, 2006). Until today this fluorophore remains the gold standard for most dye based molecular applications (Giglio et al., 2003; Monis et al., 2005; Herrmann et al., 2007; Rasmussen et al., 2007; Trantakis et al., 2010; Eischeid, 2011). As such, there is a wealth of information about SG proving extremely helpful as a benchmark for new and less well characterised fluorophors (Zipper et al., 2004; Bennett et al., 2004; Deligeorgiev et al., 2010; Trantakis et al., 2010). Affinity for high GC or AT content (positive and negative GC dependency respectively) is for example discussed for SG and several other dyes (Giglio et al., 2003; Zipper et al., 2004; Gudnason et al., 2007; Mao et al., 2007). GC dependency strengthens DNA secondary structures (Snyder et al., 2008), resulting in a reduced amplification efficiency (Giglio et al., 2003; Vaughn and Elenitoba-Johnson, 2004; Mao et al., 2007). In the context of DNA melting however it is assumed that base dependency outbalances melting plots of multiplexed qPCR. This potential influence is linked to dye-redistribution, especially if two or more products are melted in a single reaction. Redistribution is defined as the relocation of dye-molecules from an earlier melted product to a still double stranded structure thus increasing the “background” (Ririe et al., 1997; Wittwer et al., 2003; Varga and James, 2006; Wittwer et al., 2009). In the worst case a peak loss can occur and the detection of peaks at lower temperatures – such as those for primer hybrids – would be abrogated. This negative effect of redistribution most likely supported the development of high saturation dyes (Wittwer et al., 2009; Erali and Wittwer, 2010; Eischeid, 2011). In the case of multiplexed reactions, thus, proof has to be demonstrated, whether GC dependency and/or redistribution are negatively affecting the reliability of MCA.

Recently, Biotium announced a novel release-on-demand system for the new generation dye EG, which is described as the self-quenching of a dimeric dye molecule (two dye-monomers are linked with a flexible “bridge”) to reduce the background fluorescence (Figure 2).

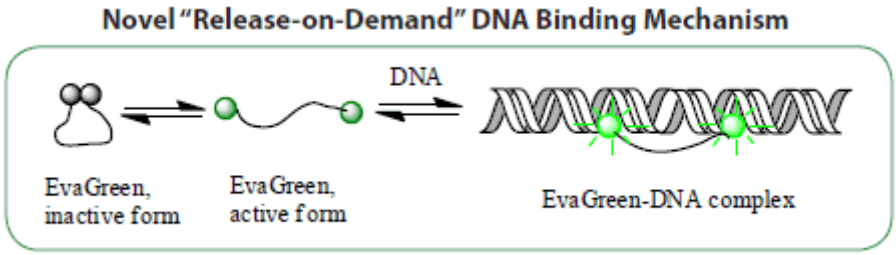

Figure 2: Promotion picture of the "Relase-on-Demand" mechanism of EG as presented on the homepage of Biotium.

EG is characterised by a novel mechanism, which is termed release-on-demand and is thought to reduce the background of qPCR.

(http://www.biotium.com/product/product_info/Newproduct/EvaGreen.asp)

Biotium reported that EG lacks relocation capacity. However, detailed information on how the release-on-demand mechanism hinders dye relocation is not available. A minor nucleotide affinity has been mentioned in 2 papers but was not described in details (Mao et al., 2007; Wang et al., 2006). The announcement of Biotium, that EG is a more reliable dye when applied in multiplex protocols, was tested in this work.

1.2 Duplex MCA – qualitative analysis employing the dyes EVAGreen, SYTO9 and SYBR Green I

Multiplexing in qPCR is often applied due to cost, time and sample limitations (van Doorn et al., 2007; Hindiyeh et al., 2005). Detection and further quantification of several targets in one reaction is mainly carried out by hydrolysis-probe based qPCR or chip assays (Hindiyeh et al., 2005; Erali et al., 2006). Dye-based multiplexing approaches are less frequently used as their results are only thought to be qualitative. Such an approach, however, can be beneficial, by combining the quantitative aspect of a probe based pathogen diagnostic assay – targeting several sequences – with the qualitative aspect of dye based MCA in a single reaction. The detection limit can be expanded and verified with the dissociation step. In other words, if a probe assay does not allow quantification below a certain copy number of a sequence it is possible to specifically detect low amplicon copy numbers by MCA. In parallel, discrimination between different amplification products including primer hybrids hence is as well assessed by MCA. In multiplex reactions the two or more peaks are true results if

detected at their specific melting temperature points (Tm's) (Varga and James, 2006). This allows reliable discrimination between for example virulent pathogens and non-virulent ones (Hochwimmer et al. 2008). Directed binding or relocation of dye molecules, however, was mentioned to potentially affect diagnostic approaches (Ririe et al., 1997; Eischeid, 2011). Additionally, the recommended or commonly used dye concentrations to saturate the reaction influence the detection of the amplified copies of different targets (Giglio et al., 2003). The dye molecule amounts, typically applied in commercially available kits, are cost effective and comparable to the standard amount of SG (1 x or 2.24 µM, respectively (Zipper et al 2004)). If the amount of the dye is insufficient to saturate (whatever the definition of this term is) two targets, this potentially would further bias results. For this work it was tested whether such effects could be described with standard methods such as MCA of purified PCR products. Three dyes (EG, SG and S9) were employed at recommended concentrations to evaluate their performance in multiplexed MCA assemblies.

Additionally, an alternative QA protocol, hybridisation, described to improve the signal-to noise ratio of high resolution melting protocols (Mendirattha et al, 2008), was studied. Here, the dye interaction with re-associating amplicon strands instead of the release after the dissociation of the double strands is examined. The kinetics of both protocols are different, as the melting drives orders to chaos in contrast to the opposite process. It is so far unknown whether such an approach improves quality assessment, although the likelihood of influences such as migrating molecules (dye molecule relocation) or strengthening of the double strands is potentially reduced. To compare dissociation and re-association protocols sequences with different melting domains were selected.

Note, that the terms dissociation and re-association were used consequently instead of melting and hybridisation in this work.

1.3 Aims of this study

dsDNA binding dyes are commonly used in qPCR setups to identify expected and co-amplified products through MCA. They are additionally utilised to discriminate multiplexed targets. Since the binding patterns of the gold standard dye SG are controversially discussed and not scrutinised for HRM capable dyes, like the 3rd generation dye EG, are studied in this work for application in MCA of multiplexed targets.

First, the performance of EG and SG was investigated in multiplexed qPCR-MCA including sequences with different GC percentage. Next, defined template copy numbers were employed to trace the saturation potential and sequence dependent binding of SG, EG and a second 3rd generation dye, SYTO9. A final experiment compared the commonly applied melting or dissociation protocol with a hybridisation protocol, which illustrates the binding of dye molecules to re-associating amplicons. This test should identify dye-based effects regarding the influence of binding moieties in the context of sequence inherent thermodynamics such as melting domains and the sequence specific Tm values.

2 MATERIALS AND METHODS

2.1 MATERIALS

2.1.1 REAGENTS AND STOCK SOLUTIONS

Agarose, Invitrogen, Lofer, A

Bromophenol blue, Merck, Darmstadt, D

DNA ladder 1 kb, Invitrogen, Lofer A

EDTA (Ethylene Diamine Tetraacetate) disodium salt, Roth, Karlsruhe, D

Ethanol (C_2H_5OH) absolute, AustrAlco Österreich, Spillern, A

Glycerol, Invitrogen, Lofer, A

Sodium Borate (SB) buffer 20x (8 g NaOH, 45 g boric acid, up to 1 l water (see below)), Sigma Aldrich, Vienna, A (Brody & Kern, 2004)

Tris/HCl ultra pure, Invitrogen, Lofer, A

Tris-EDTA buffer solution (BioUltra, for molecular biology, pH 8.0; 10 mM Tris-HCl, 1 mM disodium EDTA, pH 8.0; cat. no. 93283), Sigma Aldrich, Vienna, A

Water Molecular Biology Reagent, Sigma Aldrich, Vienna, A

2.1.2 FLUORESCENT DYES

EVAGreen®, 20 x, Biotium Inc., California, USA

Sybr® Green, 10000 x, Invitrogen, Lofer, A

SYTO® 9, 5 mM, Invitrogen, Lofer, A

2.1.3 qPCR COMPONENTS

10 x Buffer BD (800 mM Tris, 200 mM $(NH_4)_2SO_2$, Solis BioDyne, Tartu, EST

10 x Buffer A2 (800 mM Tris, 200 mM $(NH_4)_2SO_2$, 1% gelatine), Solis Biodyne, Tartu, EST

10 x Buffer B2 (800 mM Tris, 200 mM $(NH_4)_2SO_2$, 0.2% Tween-20), Solis Biodyne, Tartu, EST

dNTP mix, 20 mM each, Solis BioDyne, Tartu, EST

HOT FIREPol *Taq* DNA polymerase, 5 U/µl, Solis BioDyne, Tartu, EST

$MgCl_2$, 25 mM, Solis BioDyne, Tartu, EST

2.1.4 KITS

QIAquick PCR Purification Kit, Qiagen, Hilden, D

2.1.5 GENOMIC DNA SAMPLES

Ovis aries, source: kidney, liver, brain, muscle, blood (XenoGenetik Biotechnologie Ges.mbH, Vienna, Austria)

Aphanomyces astaci, source: lumen (provided by Dr. Gerald Hochwimmer)

Aphanomyces frigidophilus, source: lumen (provided by Dr. Gerald Hochwimmer)

Entamoeba histolytica, source: clinical samples (provided by Dr. Michael Duchene)

2.1.6 TECHNICAL EQUIPMENT

BioPhotometer, Eppendorf, Hamburg, D

Centrifuge GS-6R, Beckman, San Francisco, USA

Centrifuge 5415 C, Eppendorf, Hamburg, D

Centrifuge 5417 R, Eppendorf, Hamburg, D

Gel Imager, Alphamanager, Alpha Innotech, San Leandro, USA

Hellma Tray Cell, Hellma GmbH & Co. KG, Müllheim, D

LightCycler 480, Roche, Vienna, A

Master Cycler EPGradient S, Eppendorf, Hamburg, D

Mx3000P^{TM}, Stratagene, La Jolla, USA

RotorGene Q, Qiagen, Hilden, D

Sequence Detection Systems, ABI PRISM^{TM} 7900HT Applied Biosystems, Foster City, USA

Spectrophotometer U-3000, Hitachi, Tokyo, JP

StepOnePlus, Applied Biosystems, Foster City, USA

2.1.7 OTHER MATERIAL

Filter tips, 10/20/200/1000 µl, Greiner Bio-One GmbH, Kremsmünster, A

Filter tips, 10/20/200/1000 µl, Biozym Biotech Trading GmbH, Vienna, A

qPCR plastics:

- Microtiter plate 96-V-Thin-Wall-MT (transparent), Biozym Biotech Trading GmbH, Vienna, A
- BZO Seal Film Adhesive Optical Film, Biozym Biotech Trading GmbH, Vienna, A
- PCR SoftTubes, 0.2 ml, Biozym Biotech Trading GmbH, Vienna, A
- PCR 8-CapStrips, optically clear flat caps, Biozym Biotech Trading GmbH, Vienna, A
- 0.1 ml 4-tube strips plus caps, Qiagen, Hilden, D
- 1.5 ml reaction tubes, clear, Greiner Bio-One GmbH, Kremsmünster, A
- 1.5 ml reaction tubes, coloured, Sarstedt GmbH, Wiener Neudorf, A

2.1.8 SOFTWARE TOOLS

Copy Number Calculator:

http://www.uri.edu/research/gsc/resources/cndna.html?ngdna=15.5&bp=334&finans=4&pow_fin=11 (Staroscik, 2004)

DINAmelt: http://mfold.rna.albany.edu/?q=DINAMelt (Markham & Zuker, 2005)

Hyther™, version 1.0, N. Peyret and J. SantaLucia, Jr., Wayne State University (http://ozone3.chem.wayne.edu/cgi-bin/login/login/showLoginPage.cgi)

Meltcalc: http://www.meltcalc.de/ (Schütz and Ahsen, 1999)

MELTING: http://www.ebi.ac.uk/~lenov/meltinghome.html (Le Novére, 2001)

MELTSIM 1.0: http://www.bioinformatics.org/meltsim/wiki/ (Blake et al., 1999)

Mfold: http://frontend.bioinfo.rpi.edu/applications/mfold/ (Zucker, 2003)

OligoCalc: http://www.basic.northwestern.edu/biotools/oligocalc.html (Kibbe, 2007)

POLAND: http://www.biophys.uni-duesseldorf.de/local/POLAND/poland.html (Steger, 2004)

Primer Express 2.0, Applied Biosystems, Foster City, USA

2.2 METHODS

2.2.1 HISTORY OF TARGET DNA SEQUENCES

Primers for specific amplification of the internal transcribed spacer (ITS) region and of *CHI2*/*CHI3* sequences of *Aphanomyces astaci* and other species of the genus *Aphanomyces* were taken from Hochwimmer et al. 2009. Allelic variants of the prion protein gene *PRNP* of *Ovis aris* were kindly provided by XenoGenetik Biotechnologie Ges.mbH (Vienna, Austria). The sequence of the *Pou3F1* gene was accessed by its NCBI accession number NM_011141.2. All other sequences amplified and used to perform stand-alone Melting Curve Analysis were kindly provided by VetCore (University for Veterinary Medicine Vienna). Accessible sequences are listed in Table 1.

Table 1. Amplicon sequences employed for MCA with exact copy numbers:

Genbank accession number	length	GC content (%)	Tm value (instrument/predicted)	amplicon sequence
NM_009081.2	103	51.0	83.7/80.8	cgaaaacctgccacttcttatgtgaggaccaccatc aacaagaatgctcgggctaccctcagcagcatcag acacatgatccgaaagaacaagtaccgccctg

XM_651318.2	111	40.0	78.2/77.2	gctccagatgaccgtgctttattaatgtatactagtgg aacaactggaacacctaaaggtgttgcattaacata tcgtaatttatcagcgtcttcttcttctctgtggatg
NM_001164572.1 NM_133741.2	71	56.0	81.2/79.2	gcgatgagtacgatgcccctgcagtagacatatgg agcctgggcgtgatccttttcatgctggtgtgtggg
JQ434694.1	80	35.0	76.1/74.2	tttcgcaagaagccgatgtacttttaatcccttcttaa ataacatactgataaacttagccgtcagaaatgata gcttgt
XM_646286.2	136	32.0	77.5/76.2	agagtggagttttagtgcaaaccaagaaaattatgt tcgtgctaagtgtaaaacatgttgtagagttatttttgc ttctgattataactacaaaactaaaaaaccatttactg atgctgatgatattcgaggaga
NM_013477	99	60.0	87.5/83.3	atttcaacgtggacaatggctacttggagggattagt gcgcggcctgaaggccggggtgctcagccaggc ggactacctcaacctggtgcagtgc
NM_145558.1	110	41.0	80/77.7	gctagagctgcactttcgggtttgttgcatcggacca atattccaaaggatgttgttgattatatcatctttggta cagttattcaggaagtgaaaacaagcaatgtggc
NM_008753.4	120	57.0	86/84.3	gtggtggcctctacatcgagctcccagctggacctc tgcctgagggcagtaaggacagttttgcagctctcc tagagttcgcagaggagcaactccaggctgacca cgttttcatctgct
NM_172743.2	103	59.0	82.8	gaacgcttccgtgctcaaagagacccactggagg gcaggagggacaggagcaaggccaggtccccat acttgccagctgaggaggatgccttgtttgtcgatc
XM_650656.2	137	40.0	81.9/79.1	ttacagaaggaccaaaaactagtgttgatggtgtatt tgcatgtggggatgtatgtgatagagtatatagaca agctattgtagctgcaggaagtggttgtatggcagc cttaagctgtgaaaaatggcttcaaact
XM_650090.2	73	45.0	81.5/76.2	tcactattgttaacattgatgactgtgtcgcttgcggt gcctgttctggaacttgcccacaaagtgttcttga
XM_649311.2	76	39.0	78.3/74.1	ctagaggatggtatcctggacaagaaaaaggaag attgttatctgatactttatttagaatgggtggagccg ctat
NM_052797.1 NM_001008724.1	89	54.0	84/81.2	tgcctcatcctgagcttggccagcacagtctggact gcagacaccggcaccacaagtgaattcatagaag caggaggagatattcgtgg
NM_016856.3	102	55.0	85.6/83.2	aatgctacttacgtgcagcctagaaggaagcagag agatgagcagctcctgacaaacgtcctggaaacgc ttcggggcgacgggaacgtgctgatagctgtg
NM_032085.1	78	46.2	78.8/76.4	caccctctcttattttggcacagcagtccaatgtag atgaattgggatgcaactaccttggtcagtcctatga gtct
NM_178510.1	68	64.7	89.1/81.5	ggggtgtgcagctcactccatcctggacgtccagc tgggcgcctgcctcgaccagcactttgaggatg

2.2.2 QUANTIFICATION OF SINGLE AND DOUBLE STRANDED NUCLEIC SEQUENCES

All samples were quantified on the Biophotometer (Eppendorf, Vienna, Austria) together with a TrayCell Cuvette (Hellma, Müllheim, Germany). The factor 10 cap was used to define total amount of DNA using a 3 µl sample aliquot. Total amount of PCR product was calculated with the online software tool OligoCalc (see 3.1.8.).

Genomic DNA of sheep blood for the second proof of principle experiment was provided by XenoGenetik Biotechnologie Ges.mbH and was previously measured.

2.2.3 PCR PRODUCT PURIFICATION

PCR products were purified with the QIAquick PCR Purification Kit (Qiagen) following the protocol of the manufacturer.

2.2.4 QUANTITATIVE REAL TIME PCR (qPCR)

2.2.4.1 Primer Design

Oligonucleotides employed in this work were either reported or designed with Primer Express 2.0 software following the in lab guidelines. Primers to amplify the *Pou3F1* sequence were provided by the Institute of Animal Breeding and Genetics (University of Veterinary Medicine, Vienna). Oligos to amplify the CHI 2/3 and ITS genes equal the sequences reported by Hochwimmer et al. 2008. Primers to amplify sequences used to perform stand-alone Melting Curve Analysis were kindly provided by VetCore (University of Veterinary Medicine, Vienna) but are restricted to the knowledge of Genomics core facility. Table 2 shows the primer sequences of this work.

Table 2: Primers used for gene differentiation and Tm-shifting assays

Primers designed for *CHI 2/3* and *ITS* gene assays (5' to 3' sequences:	
Chi-f	AACGTGTGCTTCTGGCCG
Chi-r	GGGCACCAGATGAACGAC
ITS-f	GGCTTGTGCTGGGATGTTCT
ITS-r	CATTTCTGACGGCTAAGTTTATCAGTA

Primers designed for *Pou3F1* (*Oct-6*) assay (Hofmann et al., 2010)	
Oct-6-f	AGGTCCTGTTGGAGATGATATGTT
Oct-6-rr	TTGGGAAATGAATTGTCAAGAAA

Primers designed for SNP typing of *Ovis aries* Prion protein gene codon 154 position 3:		
oPrPcod154-C(os)	GCGGGCAGGGCGGC	GGGTAACGGTACATGTTTTCt**C**
oPrPcod154-C	CGGCGGCG	GGGTAACGGTACATGTTTTCt**C**
oPrPcod154-T(os)	GCGGGC	GGGTAACGGTACATGTTTTCc**T**
oPrPcod154-T		GGGTAACGGTACATGTTTTCc**T**
oPrPcod154-f		CCTCTTATACATTTTGGCAATGACTATG

Primers designed for SNP typing of *Ovis aries* Prion protein gene codon 171 position 2:		
oPrPcod171-G	CGGCGGCG	GCACAAAGTTGTTCTGGTTACTATt**C**
oPrPcod171-G-alt	CGGCGGCG	GCACAAAGTTGTTCTGGTTACTAaA**C**
oPrPcod171-A		GCACAAAGTTGTTCTGGTTACTATc**A**
oPrPcod171-A-alt		GCACAAAGTTGTTCTGGTTACTAcA**A**
oPrPcod171-A-no		GCACAAAGTTGTTCTGGTTACTATA**A**
oPrPcod171-f		ACCGTTACCCCAACCAAGTGTA

The tail sequences are underlined. Allele specific bases are given in bold. Artificial base substitutions (ARMS) are set in small letters. (os): original tailing setup (Wang et al; Biotechniques 2005).

2.2.4.2 qPCR

The 20 µl qPCR reactions consisted of 3.5 mM $MgCl_2$, 80 mM Tris pH 8.0, 20 mM $(NH_4)_2SO_2$, 200 µM dNTPs, 200 nM of each target specific primer, 1 unit of HOT FIREPol *Taq* DNA polymerase, and 2 µl DNA. dsDNA binding dyes were employed at concentrations ranging from 0.1 to 3 x for EG, 0.064 to 1.7 x for SG and 0.5 to 5 µM for SYTO9 according to the published efficient concentrations (Giglio et al., 2003; Mao et al., 2007; Monis et al., 2005). Variations of $MgCl_2$ from 2 to 6 mM and of the template from 1 pg to 1 ng were applied. For the no template control (NTC) water was employed instead of a DNA template.

The NTC was pipetted in a room absolutely free of nucleic sequences as well as in a conventional molecular biology lab. Buffers used for Tm experiments additionally included 0.1% gelatine or 0.02% Tween-20. For detection of *Pou3F1* the DyNAmo SybrGreen Kit (Finnzymes/Fisher Scientific, Vienna, A) was additionally used.

2.2.4.3 qPCR cycling protocols

All qPCR protocols started with an initial hold at 95 °C for 15 minutes (min), followed by 45 cycles consisting of 95 °C for 15 seconds (s), 60 °C for 30 s and 72 °C for 20 s. Ramping and consecutive measurement during MCA was performed using default settings of instrument software. Performance of the inverse procedure, re-association or hybridisation curve analysis, was restricted to the Rotorgene Q instrument using the settings of the alternative end point analysis step "Hybridisation", whereas the Tm was determined after transfer of the raw data set to Excel.

2.2.4.4 Stand-alone Melting Curve Analysis

When MCA was performed without preceding amplification, the temperature profile determination was set as follows: intial hold at 95 °C for 30 s, followed by rapid cooling to 60 °C and continuous ramping and measuring (0.7 °C per step / 5 s) from 60 °C to 95 °C and a final hold for 15 s at 95 °C.

Stand-alone MCA reaction mixes of 15 µl included 1.5 mM $MgCl_2$, 80 mM Tris pH 8.0, 20 mM $(NH_4)_2SO_2$, 0.1% gelatine or 0.02% Tween20 and 4 µl of mixed PCR products. The dyes were applied at concentrations of 0.1 to 1 x EG, 0.064 to 0.64 x SG, and 1 to 5 µM S9. $MgCl_2$ was varied ranging from 1 to 5 mM. Alternative buffers included either 0.01% gelatine or 0.2% Tween-20 and a buffer containing Tween-20 ranging from 0.01 to 0.4%.

2.2.5 GEL ELECTROPHORESIS

For verification of the purity of amplified products as well as the additional secondary structure assays, PCR products were verified on a non-denaturating 1% w/v agarose gel stained with 0.05 µg/ml ethidium bromide run in 1x sodium borate (SB) buffer. DNA was visualised on Alphamanager Gel Imager (Alpha Innotech, San Leandro, USA). DNA 1 kb ladder was used for estimation of DNA fragment length.

3 Results

3.1 GC content dependency of DNA binding dyes in multiplexed MCA

The aim was to elaborate whether unwanted binding patterns such as affinity towards GC- or AT-rich sequences of fluorogenic reporter dyes applied at recommended concentrations can be described for multiplex MCA.

For the 3rd generation dsDNA binding dye EG (Biotium), absence of redistributive potential and independence of sequence composition was claimed by the manufacturer. Peer-reviewed information for this effect, however, is not available on this issue. Therefore, this work evaluated the level of sequence dependence of EG in comparison to SG/SYTO9, dsDNA binding dyes known to be sequence-dependent. First, performance of EG and SG was compared using a multiplex single-color qPCR with MCA assay targeting sequences with high and low percentages of GC nucleotides. Second, the relative level of saturation and the sequence dependence regarding binding capacities or nucleotide dependent preferences during MCA were evaluated using PCR products of known sequences. Finally, an alternative quality assessment protocol was employed, which displayed the kinetics of amplicon re-association instead of dissociation.

3.1.1. Evaluation of dye performance in a multiplexed setup

A multiplex qPCR-MCA assay used to study the performance of EG and SG when the dye concomitantly targeted a sequence of *Aphanomyces* oomycetes and a consensus sequence characteristic for the class of *Oomycetes*. Contrary to SG, parallel detection of sequences with low and high GC content was facilitated by EG (Fig. 3) down to the genomic equivalent of one cell (Fig. 4). This effect was independent of dye or $MgCl_2$ concentration or their combinations (data not shown). The lower sequence preference of EG was confirmed by two additional qPCR-MCA assays. These experiments identified that SG fostered structured GC-rich targets due to its binding preference (Figures 5 and 6). Resulting, these findings prompted a more in depth study of the dyes' capability to saturate sequences of different GC content as well as the sequence inherent dependent binding. Since competition of two targets in multiplex qPCR is common (Hein & Bodendorf, 2006) and often leads to differences in end point copy number, experiments with quantified target copy numbers were performed next.

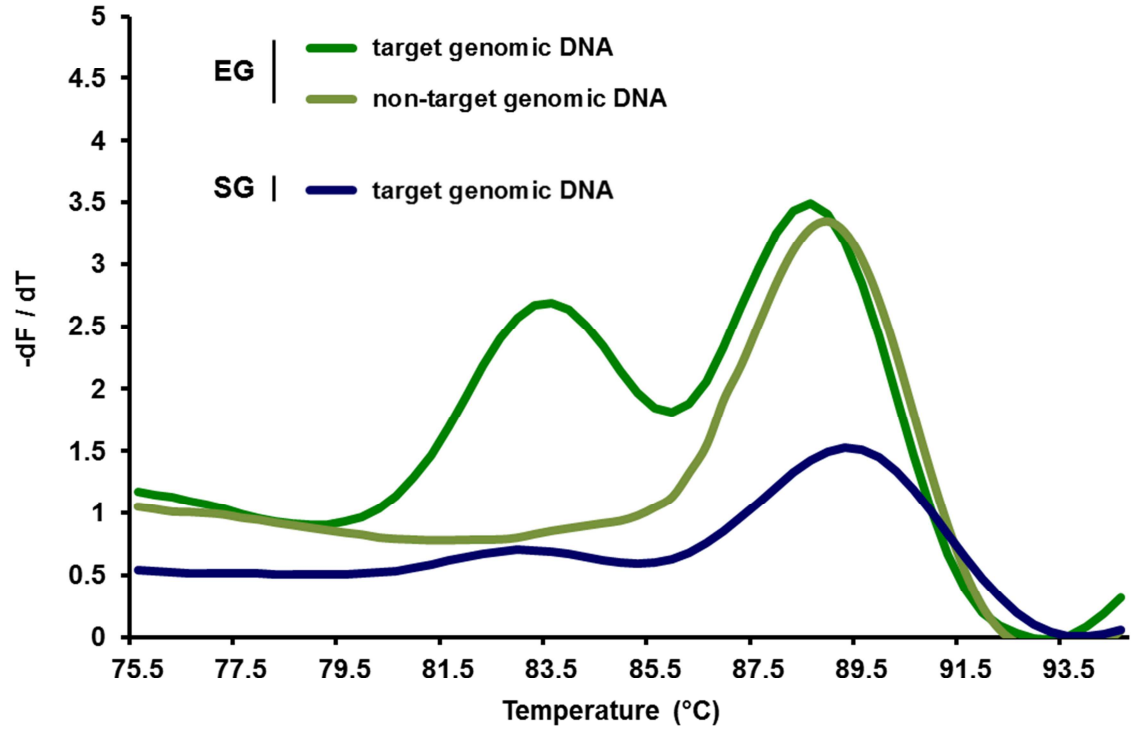

Figure 3. EG allows parallel detection of sequences with low and high GC content in clinical specimen by multiplexed dye-based qPCR-MCA.

The inability of parallel detection of different sequences by SG is explained by its preference for GC nucleotides (Monis et al., 2007). Sequences identified by the 2 peaks: *ITS2* (left) and *CHI2*/*CHI3* (right) genes. Genomic DNA was isolated from an infected crayfish specimen (template mass: 10 ng).

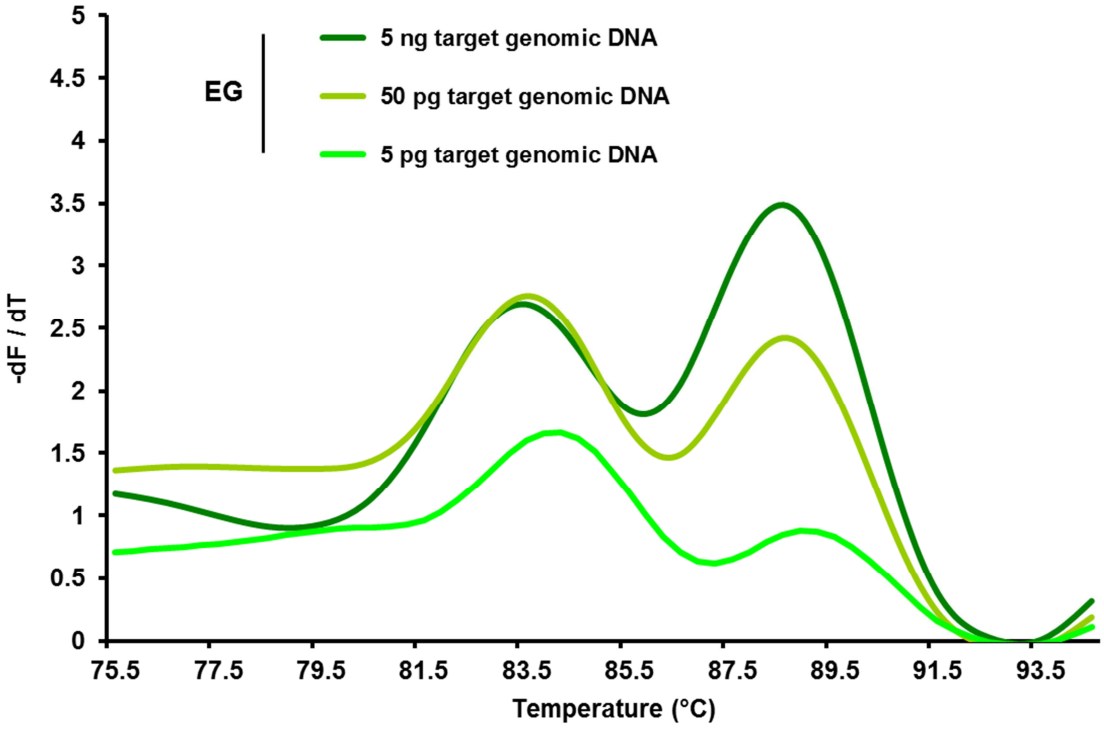

Figure 4. Serial dilution of template genomic DNA illustrates that EG allows parallel detection down to the genomic equivalent of one cell.

The limit to detect both amplification products in parallel with EG was reached employing 5 pg of genomic DNA. Similar endpoints in qPCR were achieved (data not shown).

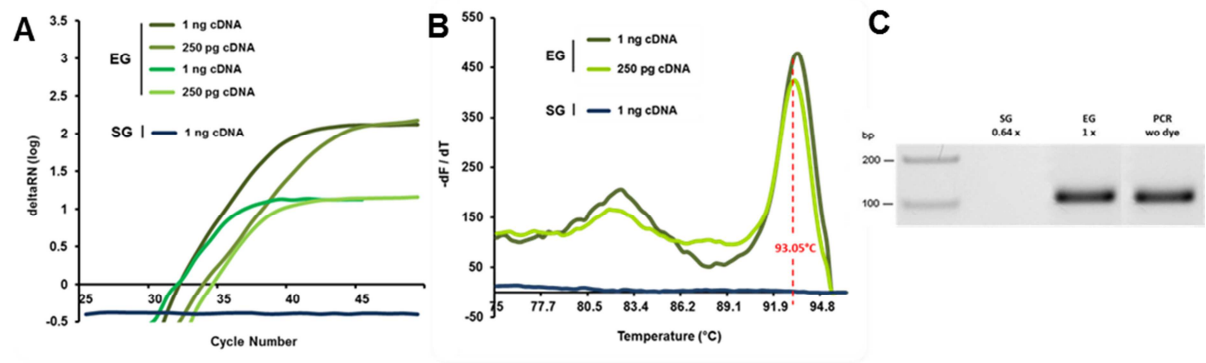

Figure 5. Inability of *Taq* DNA polymerase mediated amplification of a severely structured GC-rich sequence in the presence of SG contrary to EG due to their different sequence preferences.

A: Successful qPCR amplification of the structured GC-rich target (68% GC) only in the presence of EG; the level of endpoint fluorescence depends on the amount of dye used; **B:** MCA confirmed the expected high Tm predicted with the software tool POLAND (92 °C); **C:** Successful amplification of the sequence in the presence of EG or without any fluorophore

confirmed by gel electrophoresis (120 bp of murine *Pou3f1*); This was observed to be independent of template and dye molecule amount (1 and 0.25 ng mouse cDNA; 1 x/0.1 x EG and 0.64 x/0.1 x SG).

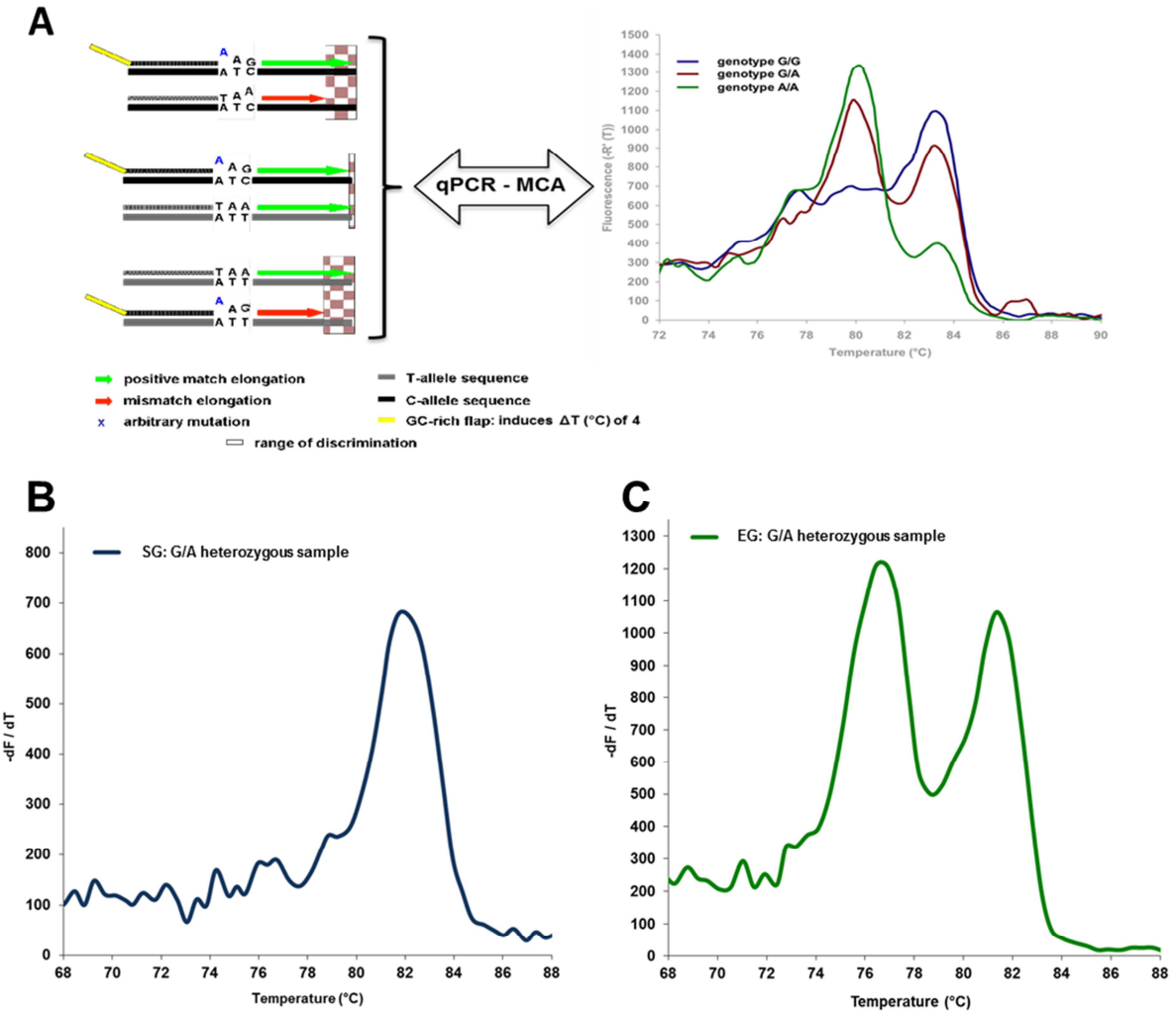

Figure 6. False negative genotyping of two alleles at a biallelic SNP site by multiplexed qPCR-MCA in the presence of SG contrary to the reliable detection by EG.

A: Melting peaks obtained by two ARMS primers (with or without an arbitrary mismatch near the primer's 3' end). The G-allele specific primer was tailed with 8 additional randomly arranged G and C nucleotides (Germer et al., 1999; Wang et al., 2006); **B:** The SG molecules are exclusively directed towards the sequence with the higher GC content leading to a false negative genotype identification, i.e. to the dropout of the A allele; **C:** The heterozygous genotype can be correctly identified with EG;

Template: 0.2 to 10 ng of genomic DNA extracted from blood.

3.1.2 MCA with defined template copy numbers to investigate directed binding

To model saturation capability and binding patterns of dye molecules, MCA of a set up containing defined template copy numbers of two selected targets with different GC contents was performed (low range 25 – 40%; high range 50 – 61% GC content; Monis et al, 2007). Target sequences had a size range from 66 to 210 bp and were arranged into pairs with similar or different length (+-10 bp, >10 and <80 bp, respectively). Additional another 3rd generation dye, S9 (2 µM), was employed to control the performance of high saturation fluorophores. Note, that the lower molar concentration of EG in a 1 x compared to 1 x SG application was ignored, since the molecular structure of EG is not yet disclosed. Higher concentrations of the latter dye were not analysed due to the putative conflict of intermolecular quenching mediated by FRET which potentially causes different signal to noise ratios (Fig. 7).

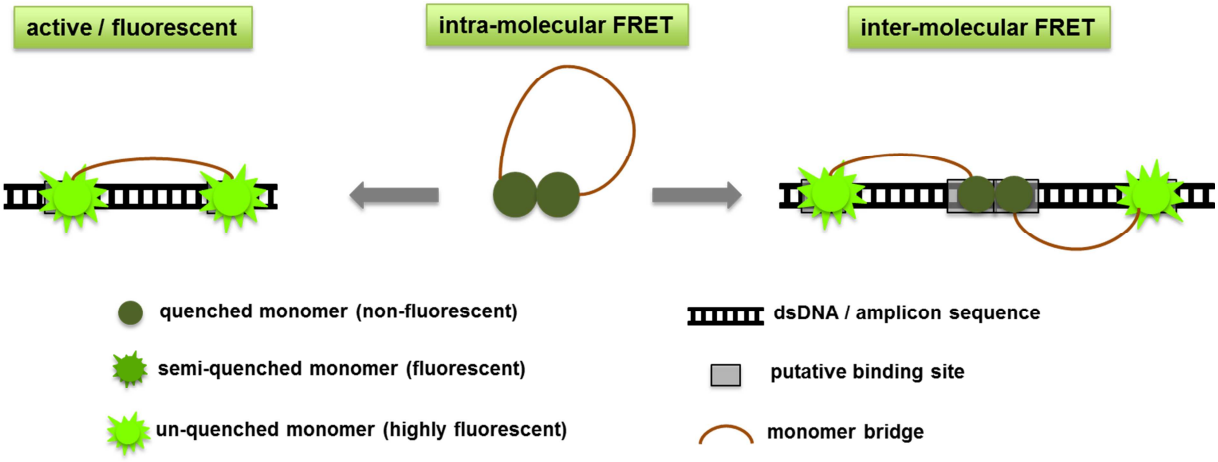

Figure 7. Inter-molecular quenching mediated by FRET potentially affects the fluorescence strength of EG at saturating concentrations.

Higher concentrations of EG increase the number of bound molecules per sequence. Due to the dimeric structure of this fluorophore, the chance of intermolecular quenching is equally increased. In this case the monomers of two dye molecules decrease each other's fluorescence similar to the effect of unbound monomers, thus affecting for example the detection of longer (> 250 bp) sequences (data not shown).

3.1.2.1 Are the dyes applied at saturating concentrations?

The first approach tested whether the recommended dye concentrations employed for a multiplexed MCA assay are sufficient to saturate the target binding sites of two amplicons. For this purpose two sequences with different GC content were mixed at different molar ratios and compared with the equimolar set up.

In the GC-rich set up, it was shown that both 1 x SG and 1x EG saturated the GC-rich sequences indicated by the uniform amplitude of the "hotter" peak (Fig. 8). In case of the increased AT-rich target we found that the distribution of the SG molecules was almost unchanged (Fig. 8). EG molecules were still able to bind to the identical target composition as indicated by a varying amplitude of the "colder" peak (Fig. 8). The recommended concentration of the alternative high saturation dye, S9, did not produce any interpretable result (see supplement). These experiments moreover indicated that the performance of all three dyes was driven by their binding preference, for example SG towards GC.

3.1.2.2 Does sequence composition direct binding of dye molecules?

Instead of a homogenous dye molecule/target ratio, the molecule distribution can be directed by the dye's binding preference, which determines the affinity towards nucleotides and the way a dye interacts with dsDNA, and binding capacity, which defines the number of putative binding regions for dye molecules within an amplicon.

The GC-affinity of SG matched peer-reviewed reports. This kinetic property triggered for example the inhibition of amplification due to interaction with secondary structure stems (Fig. 6) and indicated that the prevalent type of interaction was intercalation. 1 x SG potentially allowed saturation of two sequences, but the "colder" peak was occasionally annihilated by noise, as the GC-rich amplicon presents more binding moieties for its molecules (Fig. 8). SG, thus, preferred intercalation in GC, probably followed by binding the minor groove of less preferred targets (Giglio et al., 2003). The opposite pattern was identified for S9, whereas 2 µM of this dye were insufficient to saturate two amplicons (see supplement and data not shown). Intercalation or combined interaction types equal to SG were not defined. A different performance, however, was observed for EG. Figure 8 shows a fluorescence maximum of the "colder" peak in the equimolar mix (ΔFI). This value increased if the GC-rich target was less abundant and equally decreased if the AT-rich target was less abundant (ΔFII). In this case the fluorescence value of the "hotter" peak did not change, while it decreased with a lower difference (ΔFIII) in the opposite mix compared to ΔFII (Fig. 8). Relation of both decreased peaks, however, identified the AT-rich target peak to again outmatch the GC-rich one with

almost the same difference as it was for the equimolar setup. These findings and the solid performance during the earlier multiplexing experiments indicated that EG did not prefer any target (Fig. 3, 4, 5 and 8, respectively) and that a 1 x unit was insufficient to saturate two targets (Fig. 8). The constant fluorescence maximum of the “hotter” peak was best explained with a quenching effect that covered an achievable homogenous fluorophore distribution. EG, thus, seems to avoid binding preference, but the sequence potentially affects the emission of its dimeric molecules. Evidence how EG interacts with dsDNA and if any of the three dyes multiply bound the employed sequences was not given.

Relocating dye molecules, however, are a presumed kinetic property during dissociation, but this was not traced with the performed experiments. Since other kinetic properties additionally were found to affect MCA, an alternative to the common dissociation protocols, termed re-association, was evaluated next.

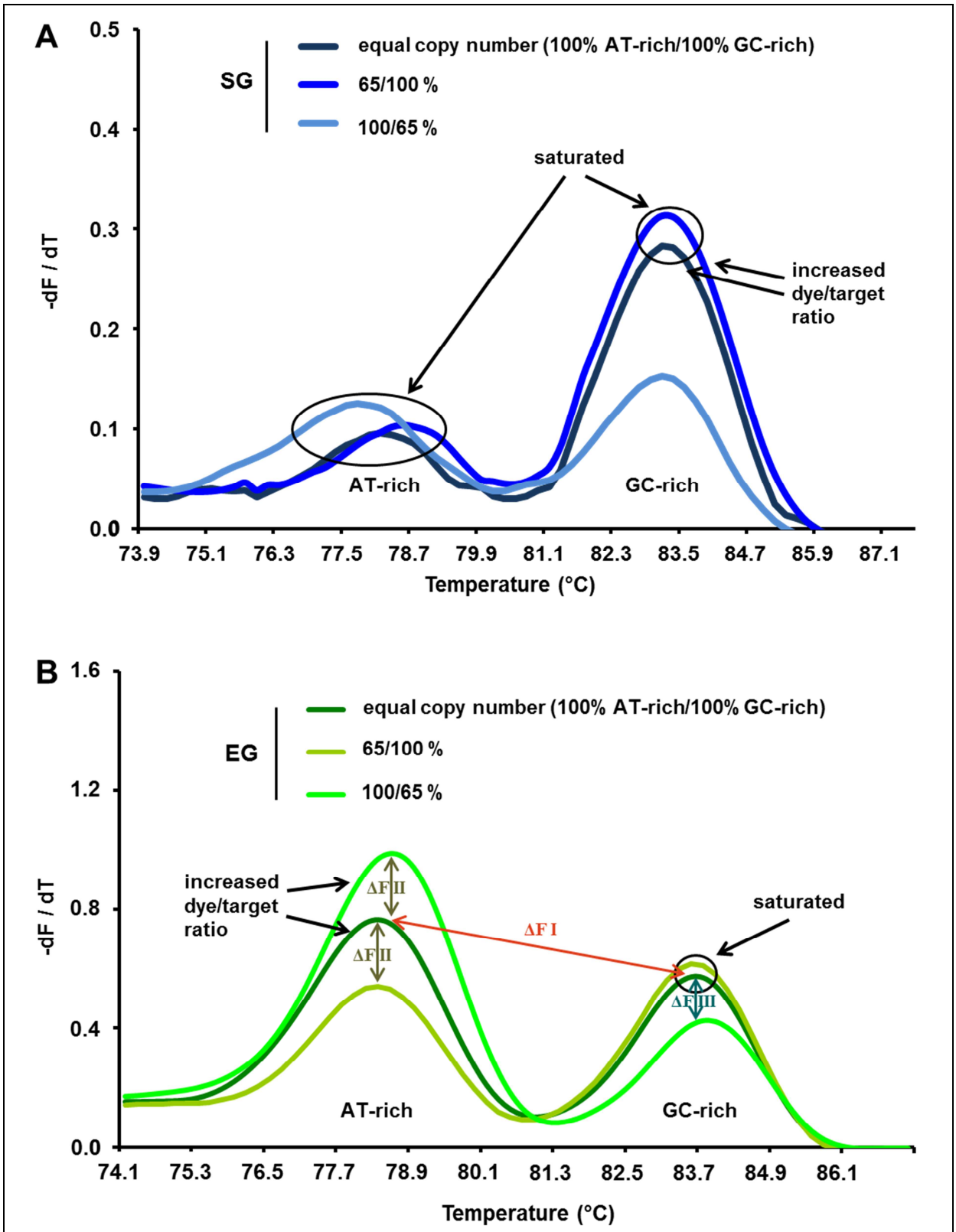

Figure 8: EG performs independent of a distinct base preferences but its recommended concentration for qPCR-MCA protocols is not sufficient to saturate two targets.

A: 1 x SG is sufficient to saturate two targets in a multiplexed MCA of sequences with identical length, indicated by two stable peaks; the higher amplitude of the GC-rich amplicon points to

preferred intercalation in GC-rich spots; the "colder peak is detectable if SG molecules are left to bind the minor groove (Giglio et al., 2003)

B: 1 x EG is not sufficient to saturate all putative binding sites of multiplexed AT- and GC-rich targets; evaluation of the different fluorescence maxima (ΔFI – III) indicates that this dye avoids preferential binding and that the height of the "hotter" peak only does not increase because of quenching effects of the dimeric EG molecule; the difference of fluorescence ΔFI between the peaks of the 100/100 % setup almost equals the difference of the peak height if both amplicons are less abundant; the fluorescence maxima of the colder peak equally change if the GC- or the AT-rich sequences are less abundant (ΔFII); the reduced difference between 100 and 60 % of the GC-rich amplicon (ΔFIII) is due to sequence dependent quenching effects.

3.1.3 Can the dissociation and the re-association of an amplicon be differentiated?

Quality assurance of dye based qPCR is typically performed by monitoring amplicon dissociation and determination of melting temperature (Tm). We as well studied the opposite process, the re-association of the amplified strands.

The appreciable difference between a dissociation and a re-association protocol was obvious for two ~200 bp long amplicons stainedwith EG. The two peaks in figure 9 indicate the presence of a co-amplified product, which, nevertheless, was not detected by gel electrophoresis (data not shown). With the prediction tool POLAND (Steger, 2004), it was predicted that both sequences contain two melting domains due to the uneven spread of the Tm regulating G and C nucleotides (Fig. 9). In contrast to dissociation the re-association protocol defined a narrow plateau, which was highly identical to the POLAND output ($\Delta T_{dissociation}$ = 4.5 °C and $\Delta T_{re\text{-}association}$ = 2.5 °C, respectively; Fig. 9). Similar results were obtained for another HRM compatible dye, S9, while SG-based reactions failed melting for unknown reason (data not shown, respectively).

Furthermore, the curve's climaxes, which display the amplicon Tms, were highly different between both protocols (~83 and 78.5 °C of the hotter peak). Retrospectively it was shown that different buffer compositions and the dye concentration altered the Tm of MCA (see supplement). Such setup dependency is not covered by predictive tools based on the nearest neighbour algorithm (Breslauer et al., 1986; Tostensen et al., 2003). The calculated Tm values (Tm_{calc}) of various sequences did not coincide with the MCA derived values (ΔT = ±3 °C; Table 3). Correlation was only clearly visible with re-association points (ΔT = ±0.5 °C; Table 3). Such matched prediction profiles ease for example the quality control of diagnostic assays, while outliers call for additional investigation. To summarise, the reassociation analysis allowed Tm without interference by the specific binding moieties of dsDNA interacting dyes.

Additional studies may prove re-association protocols generally to be superior for the quality assurance of dye based qPCR approaches.

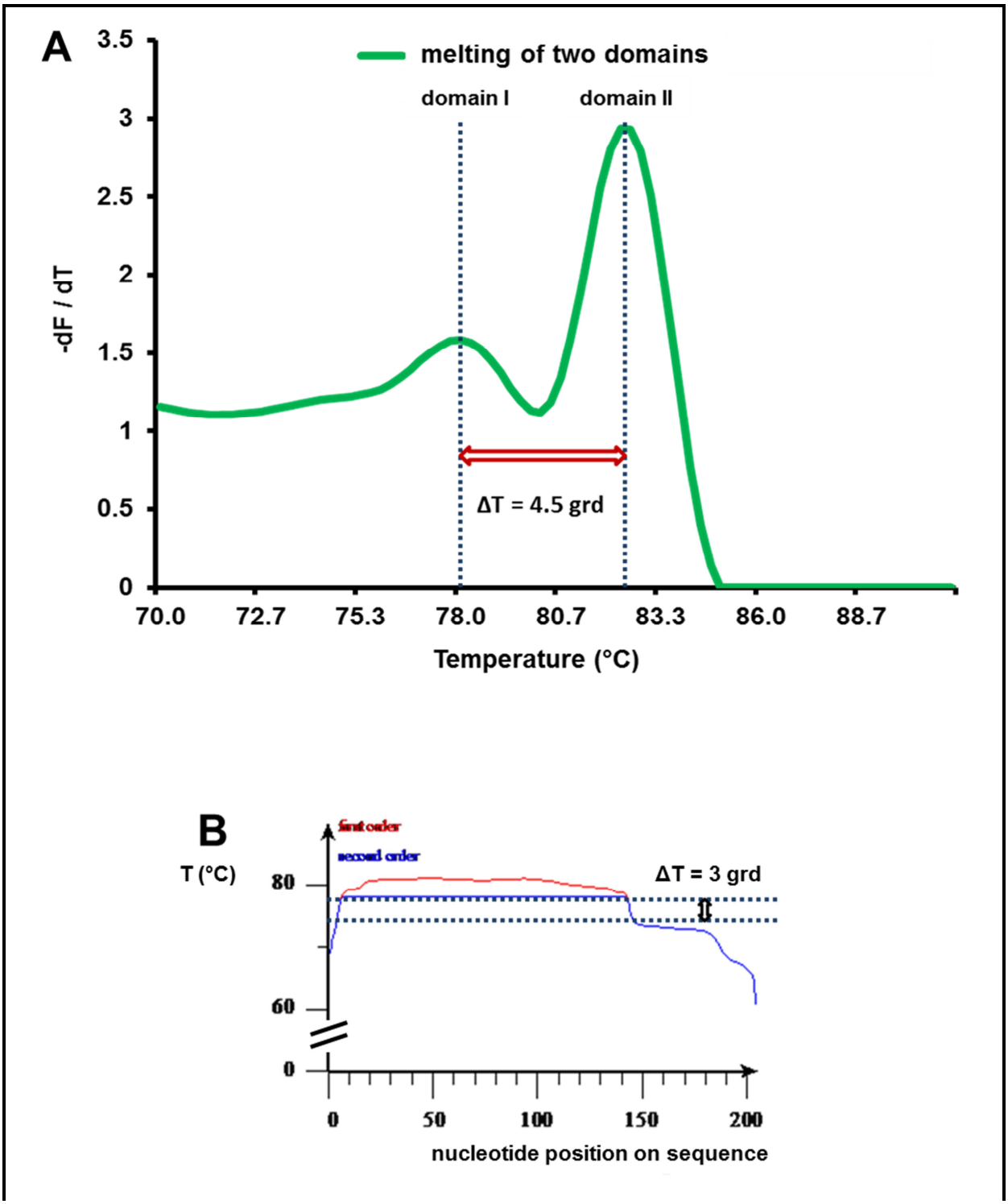

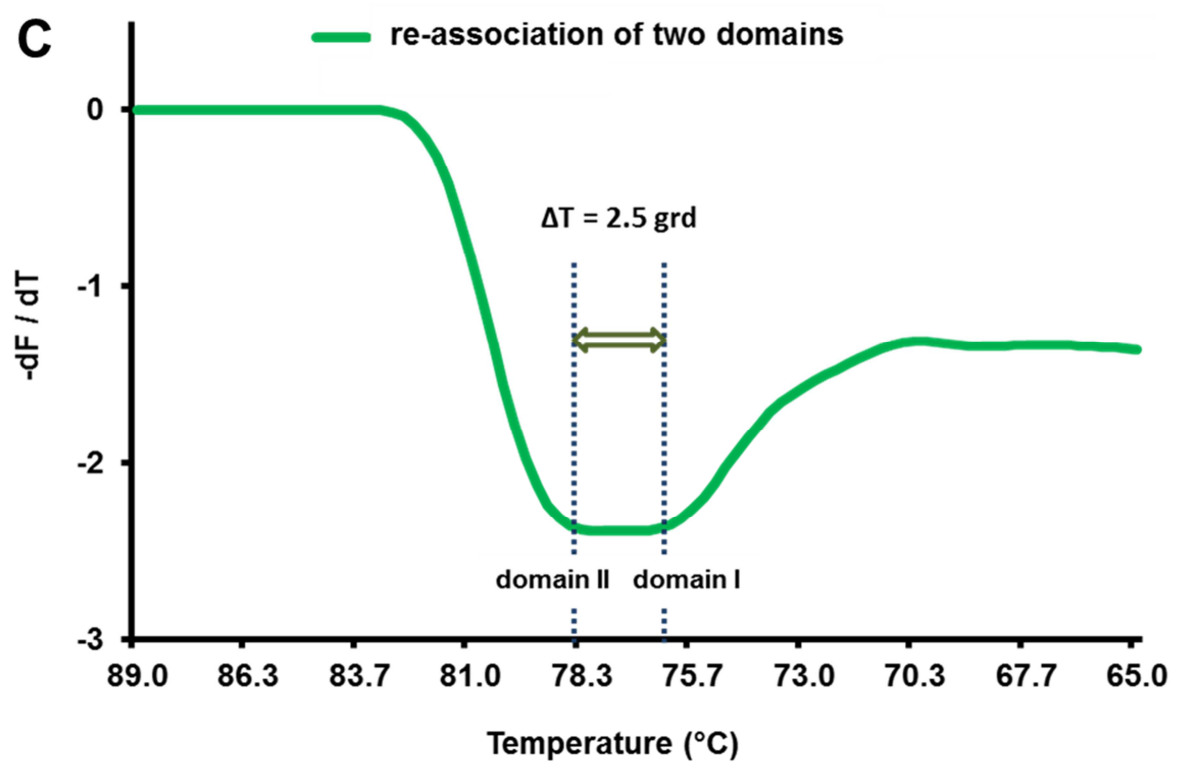

Figure 9. Re-associating amplicons allows reliable displaying of the thermodynamics of a sequence with two melting domains.

A: The derivative MCA plot of an amplicon with two melting domains implies amplification of two different sequences; **B:** Analysis of the sequence with the DNA heat map prediction tool POLAND proposes two melting domains; **C:** After derivation of the raw plot of a re-association curve, the interacting dye molecules present a narrow plateau, which equals the heat map of the POLAND algorithm;

Template: 5 ng of mitochondrial DNA extracted from liver;

Table 3. Tm prediction with nearest neighbour calculation does not match the measured melting point of dissociation protocols, but the measured re-association point of hybridisation protocols.

GenBank accessions	bp	% GC	melting domains	Tm NN (predicted)	Tm MCA	Tm RCA	POLAND
JF286601	217	32.3	1	78.2	82.5	**78.6**	78.0
JF286601 like	205	33.7	domain I 2 domain II	77.8	78.0 80.3* 82.5	**76.0** **77.2*** **78.3**	76.6 78* 79.6
NM_018184.2	179	48.7	1	82.3	85.4	**82.7**	82.6
NM_001244585.1	150	39.0	1	79.9	84.2	**79.5**	80.4
NM_010180	142	56.0	1	84.1	87.5	**83.9**	85.0
NM_000988.3	126	57.0	1	84.4	87.9	**85.3**	85
NM_207219	96	53.0	1	80.7	84.0	**81.3**	81.2
XM_650090.2	73	45.0	1	76.2	81.5	**77.1**	76.6
NM_008375	71	56.0	1	78.1	83.0	**78.9**	78.0
NM_178510.1	68	64.7	1	81.5	89.1	**83.1**	84.0

Tm NN: melting point predicted with nearest neighbour calculation

Tm MCA: measured melting point of melting curve analysis

Tm RCA: measured temperature point of re-association curve analysis

POLAND: prediction using the graphical result of the POLAND heat map tool (see supplement)

*: mean of the Tm values of domain I and II

4. Discussion

The application of the 3rd generation, HRM compatible dye EG to discriminate multiplexed targets by MCA was evaluated and compared to the performance of the standard qPCR dye SG. The applied reference multiplex qPCR-MCA setup already indicated that the quality of the results varied depending on the fluorogenic molecule employed. While EG enabled parallel detection of two targets for any chosen setup, SG poorly performed on the reference and two proof of principle approaches. Missing peaks and inhibition of the PCR in case of SG led to incorrect results after the dissociation stage. This confirmed reports that characterise SG to have binding preferences preventing a homogenous dye molecule distribution that is independent from the GC content of a sequence and binding kinetics (Giglio et al., 2003; Monis et al., 2005; Mao et al., 2007; Rasmussen et al., 2007; Eischeid, 2011). Both parameters reportedly are linked (Giglio et al., 2003; Krugh et al., 2004) and may affect saturation of two targets in MCA although a dye can interact with the target in multiple kinetic modes (Giglio et al., 2003; Dragan et al., 2010). These different patterns are outer and minor groove binding or intercalation, whereas the intercalation may cause a more severe influence due to integration within the double strand (polymerisation; Zipper et al., 2004; Eischeid, 2011). Therefore stand-alone MCA experiments were performed with EG, SG and another 3rd generation dye, S9, to target their capability of saturation and their binding preferences. Although the expected result was that neither dye was saturating, these experiments interestingly came up with the result that just SG in contrast to the HRM compatible dye was saturating if employed at recommended or reported concentrations. Additionally the approach revealed that the performance of all three fluorophores was indeed sequence dependent. SG and S9 molecules for example were able to interact at higher relative molecule numbers with strands composed of their preferred bases. In the case of SG, the effect of its preference caused almost a total GC-directed shift of its molecules. This confirmed the findings of Giglio et al. (2003), describing SG to preferentially intercalate and saturate GC-rich sequences. The less preferred target is detectable due to minor groove binding of a few free molecules mimicking saturation as described here (Fig. 8). Saturation of multiplexed targets however will be prevented, if too few dye molecules are left to interact with the less-preferred AT-rich (“colder”) sequence. A reduced copy number of the colder sequence, due to e.g. lower efficiency of its amplification, increased this negative effect. Moreover, employing a primer with an added tail of just 6 GC nucleotides to artificially “GC-enrich” amplicons of one (of two identical) target sequence(s) equally caused an almost

complete shift of the SG molecules (Figure 5). The inherent SG characteristics, thus, irritated the reliability of this multiplexed SNP-typing approach. And, the binding preference of SG on the other hand already influenced the preceding enzymatic amplification step by strengthening the hydrogen bonds of the DNA helix. An equally concrete explanation was not found for S9, which was identified to prefer AT-rich sequences (see supplement). 2 µM of this dye were insufficient to saturate two targets, but determined a fluorescence maximum of the "colder" peak independent of a less abundant AT- or GC-rich target. A definition of its binding kinetics was not traced and binding kinetics equal to SG and intercalation can only be assumed.

Such imbalances, however, were avoided with EG. In contrast to the few published statements, the performance of EG in the end was evaluated not to depend on base and hence binding preference. The stand-alone melting experiments initially indicated that a 1 x unit was insufficient to saturate binding sites of two targets, as only the "hotter" peak did not change (Fig. 8). Due to this single "saturation" effect, GC-directed binding of EG was assumed, while the AT-rich sequences allowed for more interaction sites (Fig. 8). EG nevertheless is a self-quenching dimeric molecule. This unique superstructure reduces the background but was suspected to potentially interfere with real-time detection (Fig. 7). A comparison of the fluorescence maxima of the "colder" and "hotter" peaks at equal target numbers (100 vs. 100 and 60 to 60 %, respectively) confirmed this idea. The same difference was given independent of the overall amplicon number (Fig. 8). The peak height of the GC-rich sequences however did not change if the AT-rich sequences were less abundant. This effect specifically for GC-rich templates might result from self-quenching of the dye molecules abrogating multiple dye molecule attachment or bending of the target reducing the emission per single dye molecule and further attachment. Instead of the sequence composition the different electron cloud of GC-rich sequences is more likely reasoned to cause this pattern. EG molecules, thus, distribute independently of a distinct base preference, but the GC content still affects the performance of this dye. This unique attribute, however, did not severely out-balance the overall performance of this dye allowing solid simultaneous detection of two targets in any of our setups. This makes EG – even a 1 x, not saturating unit – a more reliable choice for multiplexed qPCR-MCA setups compared to SG, for which a distinct base preference influences the consistency of the result. Results for SG point out that the assay design needs careful, "dye dependent" planning. For a conventional two-target-multiplex qPCR-MCA approach, typically the GC content of one target is < 50% and the one of the other > 58% to yield a ΔTm of ≥2.5 °C for discrimination. First of all, the amplification kinetic of a

multiplexed reaction stemming from two assay designs is unpredictable as one target could be more efficiently amplified than the other causing divergent copy numbers at the end point of PCR. This divergence is additionally increased if the relative amount of the different dNTPs is not adjusted to the assay needs, the initial copy numbers are unknown or if the dye and enhancers already influence the amplification process. Employing SG for a multiplexed reaction where the GC-rich amplicons are more abundant at the end point provokes a peak loss of the colder (AT-rich) amplicon after MCA. The recommended amount of SG is not sufficient to saturate both targets. The small number of dye molecules left to interact with the colder amplicon, however, is further reduced in fluorescence by noise and was shown not to relocate, as the maximum saturation capacity of the hotter amplicon was already reached (Figure 8). In other words, redistribution is no threat for SG based setups, whereas the commonly applied assay designs are. Instead of the commonly established multiplex design (amplicon 1: <50% GC and amplicon 2: >58% GC, respectively) the GC content of both amplicons should be above 50% and the Δ% GC of > 9 must be retained to maintain the ΔTm of > 2.5 °C, necessary for discrimination of two targets. Determination of an amplicon sequence with a GC content of more than 60 %, however, is not trivial, given the limitations/rules of primer designs and potentially increased single-strand amplicon structure, shown to inhibit amplification in the presence of SG. Changing the assay design thus can support the detection of both amplicon-peaks, as the number of SG molecules interacting with the colder amplicon increases, but invariably complicates the design strategy. In case of EG, the assay design does not matter. This especially since EG and S9 based reactions can be further enriched with dye molecules for complete saturation, while higher concentrations of SG inhibit amplification (Eischeid, 2011).

All these interpretations nevertheless ignored the potential of dye molecule relocation from earlier to later melting targets, which is reported as a latent threat of multiplexed systems (Wittwer et al., 2003). According to our findings, only S9 is likely subjected to redistribution at recommended concentrations, as it prefers “colder” AT-rich sequences and does not saturate the second target of higher GC content. The distribution of EG or SG molecules more likely happens and ends at the colder “starting” plateau of the melting step, or during the cooling down from a 95 °C dissociation step prior to MCA, where either double stranded amplicons or re-associating strands are present. Negative attributes, such as directed distribution, and effects caused by other PCR additives although still affect the resulting MCA plots.

In contrast to the putatively biased analysis of the progressive dissociation of several amplicons, the inverse procedure – detection of re-associating amplicons when cooling down from a 95 °C heat step – should abolish the negatively described effect. Such re-association protocols, also termed hybridisation curve analysis, reduce dye-based influences. They potentially avoid relocation, interactive strand strengthening and provide an improved view of binding affinities without wrong characterisation of the melting kinetics of sequences. Due to the fact that the dye molecule/target interaction is caused and not terminated, this method allows the unbiased imaging of sequence immanent melting patterns, such as two melting domains. Additionally it was shown that the Tm of re-associated amplicons almost equalled the "nearest neighbour"-based predictions. Tm values identified by MCA in contrast were significantly increased due to enhancer mediated dye/target interaction. While the prediction of dissociation curve based Tm's can be optimised by setup dependent modifications of reviewed algorithms (Mackey & Landt, 2004), it is not possible to reduce the influence of the dyes and enhancers on dissociation. This influence is only abolished by measuring the cooling and hence re-association of amplicons. Thus the statement of Mehndiratta et al (2008) that the kinetics of dissociation and re-association being different is true but has to be focussed on the fact that the dyes cause this difference.

A final reflection, however, aims at the typically reported terms preference and saturation (cits!!). It was shown that a superficial use of both attributes is not sufficient to describe the performance of any dye. The basic understanding of the term saturation, for example, is coverage of all putative binding sites per sequence and the total number of sequences. We defined that covering of binding sites depends on the attributes of any dye. This especially since a 1 x unit of SG indeed allowed saturation of two targets, but saturated its intercalation "hot spots" above all. A 1 x unit of EG on the other hand is sufficient to describe two targets by qPCR-MCA. The described self-quenching effect of this dye, however, does even not conduce to enriching a reaction with its molecules as the plot image might not improve. 1 x EG, thus, is sufficient to reliably interpret multiplexed MCA without the need to further enrich a reaction and is as such used at an already saturating level, since at least "first order" binding sites (as more potential interactions can be assumed as for PG or SG) are covered. Moreover, this dye was evaluated to avoid directed binding because of a base preference. Its performance nevertheless was influenced by sequence patterns. A superficial interpretation that this is due to AT- or GC-affinity although is not fitting. Even for SG base preference calling is misleading. Its interaction kinetics drive the binding order, which may be due to its own or the sequence moieties like different electron clouds or stretching mechanisms.

To conclude, saturation even is achieved at lower dye input levels, if the amount is sufficient to determine the multiple peaks of a multiplex qPCR-MCA setup. The order of interaction preferences is as important as base preference calling. Reporting the different dye specific attributes thus is necessary to allow for appropriate dye selection in the context of the experimental setup. The given information, however, is scarce and intercalation typically is used as a reference instead of the more objective term "dsDNA binding", if the binding activities are not disclosed yet. A brief summary of disclosed and unknown attributes of some dyes is given in table 4. Because of these patterns, a dye moreover might interfere with other detection formats in a mixed setup. MGB-probes mixed with SG for example might compete with dyes for the minor grooves, which affects the overall setup performance. Re-association curve analysis, finally, allows a more concise characterisation of the amplified targets and hence quality control for the performed assays than dissociation curve analysis. And, regarding the dye selection for multiplex qPCR-MCA experiments, only EG allowed a solid performance due to avoiding redistribution or preferential binding as claimed by Biotium and is hence valuable for future experiments.

Table 4. Disclosed and unknown attributes of the "first starters" EtBr and SG, the high saturation dyes Bebo, EG, S9 and PicoGreen.

dsDNA binding dyes	structure definition	moleculare structure disclosed	binding patterns	base preference	saturation limits	redistribution* capacity	molecular applications	remarks
EvaGreen® (EG)	dimeric: two bridged dye molecules	unknown	unknown**	no preference	high saturation (> 3 x)	no (this work)	qPCR-MCA, HRM	dimeric structure may cause sequence dependent self quenching effects (this work)
Sybr® Green (SG)	single dye molecule	Zipper et al., 2004	intercalation/ minor groove binding (Giglio et al., 2003; this work)	G/C (intercalation; this work)	> 1.5 x inhibit PCR	no (this work)	qPCR-MCA, HRM	biologically risky; not useful for multiplex qPCR-MCA without enhancers
SYTO® 9 (S9)	single dye molecule	Deligeorgiev et al., 2008	unknown (this work)	A/T (this work)	high saturation (> 4 µM)	likely (this work)	qPCR-MCA, HRM	
ethidium bromide (EtBr)	single dye molecule	e.g.: Liebmann et al., 1977	intercalation (Monaco, 2010)	G/C (intercalation)	unknown	unknown	gel staining	biologically risky
PicoGreen (PG)	single dye molecule	Dragan et al., 2010	intercalation/ minor groove binding/ outer binding (Dragan et al., 2010)	unknown	unknown	unknown	qPCR?, RNA staining	
BeBo	single dye molecules (can combine to dimers)	Karlsson et al., 2003	minor groove binding	unknown	high saturation (> 4 µM)	unknown	qPCR-MCA, HRM	

*: redistribution capacity defines whether dye molecules shift from the colder to the hotter target of multiplex qPCR-MCA;

**: A/T preference is assumed in literature (Mao et al., 2007), but not claimed by Biotium; here, EG was avoiding preferential binding;

4.1 Conclusion

In summary, sequence dependent binding patterns were identified for all dyes employed. The described threat of dye redistribution, that is the drift of dye molecules from sequences melting at lower temperature to those melting at a higher temperature, was excluded for MCA with EG and SG. For AT-affine dyes like S9 this effect has to be assumed if used at low, recommended concentrations, though without negatively affecting the imaged two-peak plot. Further negative effects only were described for SG, whereas the commonly applied assay design was identified as the decisive factor hampering the use of this dye for conventional multiplexed qPCR-MCA setups. Future work will show whether a change of assay design (two rather GC-rich targets), adjustment of the relative dNTP concentrations or cycle number adjustment will allow reliable, qualitative determination of two targets in one reaction with the gold standard, SG. Nevertheless, only the "claimed" attributes of EG to avoid redistributive or preferential kinetics allowed an almost balanced spread of the dye molecules between targets of differing GC content and provided best results for parallel detection of two target sequences in a multiplexed qPCR-MCA approach even at low and sub saturation levels. This argues against the need for a high saturation employment, as is generally recommended for the 3rd generation dyes. It is of higher importance to disclose any dye's binding patterns and optimise assay design rather than to increase the number of dye molecules. Employing re-association protocols on such amplicons, however, renders such discussions void as it was positively evaluated for the quality control of PCR assays. Compared to dissociation (MCA), RCA is a better choice to define temperature points accurately that equal predicted values without variability caused by a dye or unknown buffer components. This is extremely useful, if proprietary reaction mixes are used. Unfortunately, only few real-time PCR instruments allow progressive measurement during cooling/hybridisation.

This work indicates that MCA used to confirm an amplicon sequence is not trivial, but holds potential for improvement.

5 References

Afonina, I., Ankoudinova, I., Mills, A., Lokhov, S., Huynh, P., Mahoney, W., et al. (2007). Primers with 5′ flaps improve real-time PCR. *BioTechniques*, *43*(6), 770-774.

Bengtsson, M., Karlsson, J. H., Westman, G., & Kubista, M. (2003). A new minor groove binding asymmetric cyanine reporter dye for real-time PCR. *Nucleic Acids Research*, *31*(8), 45e-45.

Bennett, T. N., Paguio, M., Gligorijevic, B., Seudieu, C., Kosar, A. D., Davidson, E., et al. (2004). Novel, Rapid, and Inexpensive Cell-Based Quantification of Antimalarial Drug Efficacy. *Microbiology*, *48*(5), 1807-1810.

Biver, T., Boggioni, A., Secco, F., Turriani, E., Venturini, M., Yarmoluk, S., et al. (2007). Influence of cyanine dye structure on self-aggregation and interaction with nucleic acids: a kinetic approach to TO and BO binding. *Archives of Biochemistry and Biophysics*, *465*(1), 90-100.

Blake, R.D. & Delcourt, S.G. (1998). Thermal stability of DNA. *Nucleic Acids Research*, 26(14), 3323-3332.

Blake, R. D., Bizzaro, J. W., Blake, J. D., Day, G. R., Delcourt, S. G., Knowles, J., et al. (1999). Statistical mechanical simulation of polymeric DNA melting with MELTSIM. *Bioinformatics*, *15*(5), 370-375.

Breslauer, K. J., Franks, R., Blockers, H., & Markyt, L. A. (1986). Predicting DNA duplex stability from the base sequence. *Proceedings of the National Academy of Sciences*, *83*(June), 3746-3750.

Brody, J. R., Kern, S. E. (2004). Sodium boric acid: a Tris-free, cooler conductive medium for DNA electrophoresis. *Biotechniques*, 36(2), 214-6.

Burgstaller, J. P., Schinogl, P., Dinneys, A., Müller, M., Steinborn, R. (2007). Mitochondrial DNA heteroplasmy in ovine fetuses and sheep cloned by somatic cell nuclear transfer. *BMC Developmental Biology*. 7:141.

Chou, L., Lyon, E., & Wittwer, C. T. (2005). A Comparison of High-Resolution Melting Analysis With Denaturing High-Performance Liquid Chromatography for Mutation Scanning: Cystic Fibrosis Transmembrane Conductance Regulator Gene as a Model. *American Journal of Clinical Pathology*, *124*(3), 330-338.

Deligeorgiev T.G., Kaloyanova S., Vaquero J.J. (2010). Intercalating Cyanine Dyes for Nucleic Acid Detection. *Recent Patents on Materials Science*, 2(1):1-26.

Dragan, A.I., Casa-Finet, E.S., Strouse, R.J., Schenerman, M.A., Geddes, C.D. (2010). Characterization of PicoGreen Interaction with dsDNA and the Origin of Its Fluorescence Enhancement upon Binding. *Biophysical Journal*, 99(11), 3010-3019.

Eischeid, A.C. (2011). SYTO dyes and EvaGreen outperform SYBR Green in real-time PCR. *BMC Research Notes*, 4(263), pp.2-6.

Elenitoba-Johnson, K.S., Bohling, S.D., Wittwer, C.T., & King, T.C. (2001). Multiplex PCR by multicolor fluorimetry and fluorescence melting curve analysis. *Nature Medicine, 7*(2), 249-253.

Erali, M. & Wittwer, C.T., (2010). High Resolution Melting Analysis for Gene Scanning. *Methods*, 50(4), 250-261.

Eriksson, M., Karlsson, J. H., Westman, G., & Akerman, B. (2003). Groove-binding unsymmetrical cyanine dyes for staining of DNA: dissociation rates in free solution and electrophoresis gels. *Nucleic Acids Research, 31*(21), 6235-6242.

Germer, S., & Higuchi, R. (1999). Single-Tube Genotyping without Oligonucleotide Probes. *Genome Research, 9*, 72-78.

Giglio, S., Monis, P.T., & Saint, C.P. (2003). Demonstration of preferential binding of SYBR Green I to specific DNA fragments in real-time multiplex PCR. *Nucleic Acids Research, 31*(22), 136e-136.

Gudnason, H., Dufva, M., Bang, D.D., & Wolff, A. (2007). Comparison of multiple DNA dyes for real-time PCR: effects of dye concentration and sequence composition on DNA amplification and melting temperature. *Nucleic Acids Research, 35*(19), e127.

Hannah, K.C. & Armitage, B.A. (2004). DNA-Templated Assembly of Helical Cyanine Dye Aggregates : A Supramolecular Chain Polymerization. *Accounts of Chemical Research*, 37(11), 845-853.

Hein, A.E. & Bodendorf, U. (2007). Real-time PCR : Duplexing without optimization. *Analytical Biochemistry*, 360, 41-46.

Herrmann, M.G., Durtschi, J.D., Wittwer, C.T., & Voelkerding, K.V. (2007). Expanded instrument comparison of amplicon DNA melting analysis for mutation scanning and genotyping. *Clinical Chemistry, 53*(8), 1544-1548.

Hindiyeh, M., Levy, V., Azar, R., Varsano, N., Regev, L., Shalev, Y., et al. (2005). Evaluation of a Multiplex Real-Time Reverse Transcriptase PCR Assay for Detection and Differentiation of In uenza Viruses A and B during the 2001-2002 Infuenza Season in Israel. *Journal of Clinical Microbiology, 43*(2), 589-595.

Hochwimmer, G., Tober, R., Bibars-Reiter, R., Licek, E., Steinborn, R. (2009). Identification of two GH18 chitinase family genes and their use as targets for detection of the crayfish-plague oomycete Aphanomyces astaci. *BMC Microbiology*, 9(184), 1-17.

Hoebeeck, J., Speleman, F., & Vandesompele, J. (2007). Real-time quantitative PCR as an alternative to Southern blot or fluorescence in situ hybridization for detection of gene copy number changes. *Methods in Molecular Biology, 353*, 205-226.

Hofmann,E., Reichart, U., Gausterer, C., Guelly, C. Meijer, D., Müller, M., Strobl, B. 2010. Octamer-binding factor 6 (Oct-6 / Pou3f1) is induced by interferon and contributes to dsRNA-mediated transcriptional responses. *BMC Cell Biology*, 61(11), 1471-2121.

Ihrig J, Lill R, Mühlenhoff U. (2006). Application of the DNA-specific dye EvaGreen for the routine quantification of DNA in microplates. *Analytical Biochemistry*, 359(2), 265-7.

Kibbe, W.A. (2007). OligoCalc : an online oligonucleotide properties calculator. *Nucleic Acids Research*, 35(Web Server Issue), 43-46.

Le Novère, N. (2001). MELTING, computing the melting temperature of nucleic acid duplex. *Bioinformatics Applications Note*, *17*(12), 1226-1227.

Liebman, M., Rubin, J. & Sundaralingam, M., 1977. Nonintercalative binding of ethidium bromide to nucleic acids : Crystal structure of an ethidium-tRNA molecular complex. *Biochemistry*, 74(11), 4821-4825.

Liew, M., Pryor, R., Palais, R., Meadows, C., Erali, M., Lyon, E., Wittwer, E. (2004). Genotyping of single-nucleotide polymorphisms by high-resolution melting of small amplicons. *Clinical Chemistry*, *50*(7), 1156-1164.

Mackay, J. & Landt, O. (2004). Real-Time PCR Fluorescent Chemistries. *Methods in Molecular Biology*, *353*, 237-261.

Mao, F., Leung, W., & Xin, X. (2007). Characterization of EvaGreen and the implication of its physicochemical properties for qPCR applications. *BMC Biotechnology*, *7*, 76

Mehndiratta, M., Palanichamy, J.K. & Ramalingam, P. (2008). Short Technical Reports Fluorescence acquisition during hybridization phase in quantitative real-time PCR improves specificity and signal-to-noise ratio. *Biotechniques*, 45(12), 625-634.

Monaco, R.R. (2010). Capture of a Transition State Using Molecular Dynamics : Creation of an Intercalation Site in dsDNA with Ethidium Cation. *Journal of Nucleic Acids*, 2010(March), 3-6.

Monis, P.T., Giglio, S., & Saint, C.P. (2005). Comparison of SYTO9 and SYBR Green I for real-time polymerase chain reaction and investigation of the effect of dye concentration on amplification and DNA melting curve analysis. *Analytical Biochemistry*, *340*(1), 24-34.

Picard C, Silvy M, Gabert J. (2006). Overview of Real-Time RT-PCR Strategies for Quantification of Gene Rearrangements in the Myeloid Malignancies. *Methods in Molecular Medicine*, 125, 27-68.

Ponchel F, Toomes C, Bransfield K, et al. (2003). Real-time PCR based on SYBR-Green I fluorescence: An alternative to the TaqMan assay for a relative quantification of gene rearrangements, gene amplifications and micro gene deletions. *BMC Biotechnology*, 13, 1-13.

Pryor, R.J., Wittwer, C.T. (2006). Real-Time Polymerase Chain Reaction and Melting Curve Analysis. *Methods in Molecular Biology^{TM} – Clinical Applications of PCR 2nd Edition* 336: 19-32

Rasmussen, J.P., Saint, C. P., & Monis, P.T. (2007). Use of DNA melting simulation software for in silico diagnostic assay design: targeting regions with complex melting curves and confirmation by real-time PCR using intercalating dyes. *BMC Bioinformatics*, *8*, 107.

Ririe, K.M., Rasmussen, R. P., & Wittwer, C.T. (1997). Product Differentiation by Analysis of DNA Melting Curves during the Polymerase Chain Reaction, *Analytical Biochemistry 160*(245), 154-160.

SantaLucia, J.J. (1998). A unified view of polymer, dumbbell, and oligonucleotide DNA nearest-neighbor thermodynamics. *Proc. Natl. Acad. Sci. USA Biochemistry*, 95 (February), 1460-1465.

Schütz, E., & von Ahsen, N. (1999). Spreadsheet software for thermodynamic melting point prediction of oligonucleotide hybridization with and without mismatches. *BioTechniques*, *27*(6), 1218-1224.

Singer V.L., Lawlor TE, Yue S. (1999). Comparison of SYBR Green I nucleic acid gel stain mutagenicity and ethidium bromide mutagenicity in the Salmonella/mammalian microsome reverse mutation assay (Ames test). *MutationRresearch*, 439(1), 37-47.

Snyder, T. M., Tse, B.N., & Liu, D.R. (2008). Effects of template sequence and secondary structure on DNA-templated reactivity. *Journal of the American Chemical Society*, *130*(4), 1392-1401.

Steger, G. (1994). Thermal denaturation of double-stranded nucleic acids : prediction of temperatures critical for gradient gel electrophoresis and polymerase chain reaction. *Nucleic Acids Research*, 22(14), 2760-2768.

Tøstensen E, Fang L, Jenssen T-kristian, Hovig E. (2003). Speed-Up of DNA Melting Algorithm with Complete Nearest Neighbor Properties;70:364 -376.

Trantakis, I.A., Fakis M, Tragoulias S.S., et al. (2010). Ultrafast fluorescence dynamics of Sybr Green I/DNA complexes. *Chemical Physics Letters*, 485(1-3), 187-190.

van Doorn, R., Szemes, M., Bonants, P., Kowalchuk, G. a., Salles, J.F., Ortenberg, E., et al. (2007). Quantitative multiplex detection of plant pathogens using a novel ligation probe-based system coupled with universal, high-throughput real-time PCR on OpenArrays. *BMC Genomics*, *8*, 276.

Varga, A., & James, D. (2006). Real-time RT-PCR and SYBR Green I melting curve analysis for the identification of Plum pox virus strains C, EA, and W: effect of amplicon size, melt rate, and dye translocation. *Journal of Virological Methods*, *132*(1-2), 146-153.

Vaughn, C.P., & Elenitoba-Johnson, K.S. (2004). High-Resolution Melting Analysis for Detection of Internal Tandem Duplications. *Journal of Molecular Diagnostics*, *6*(3), 211-216.

Wang, J., Chuang, K., Ahluwalia, M., Patel, S., Umblas, N., Mirel, D., et al. (2005). High-throughput SNP genotyping by single-tube PCR with Tm-shift primers. *BioTechniques*, *39*(6), 885-893.

Wang, W., Chen, K., & Xu, C. (2006). DNA quantification using EvaGreen and a real-time PCR instrument. *Analytical Biochemistry, 356*(2), 303-305.

Wittwer, C. T., Reed, G. H., Gundry, C. N., Vandersteen, J. G., & Pryor, R. J. (2003). High-Resolution Genotyping by Amplicon Melting Analysis Using LCGreen. *Clinical Chemistry, 49*(6), 853-860.

Wittwer, C.T., Reed, G., Dujols;,V., Zhou, L. (2004). Amplicon melting analysis with saturation dyes. United States Patent 10/531,966; WO2004/038038.

Wittwer, C.T., Reed, G., Dujols;,V., Zhou, L. (2009). Amplicon melting analysis with saturation dyes. United States Patent 12/833,274.

Zipper, H., Brunner, H., Bernhagen, J., & Vitzthum, F. (2004). Investigations on DNA intercalation and surface binding by SYBR Green I, its structure determination and methodological implications. *Nucleic Acids Research, 32*(12), e103.

Zuker, M. (2003). Mfold web server for nucleic acid folding and hybridization prediction. *Nucleic Acids Research, 31*(13), 3406-3415.

6 SUPPLEMENT

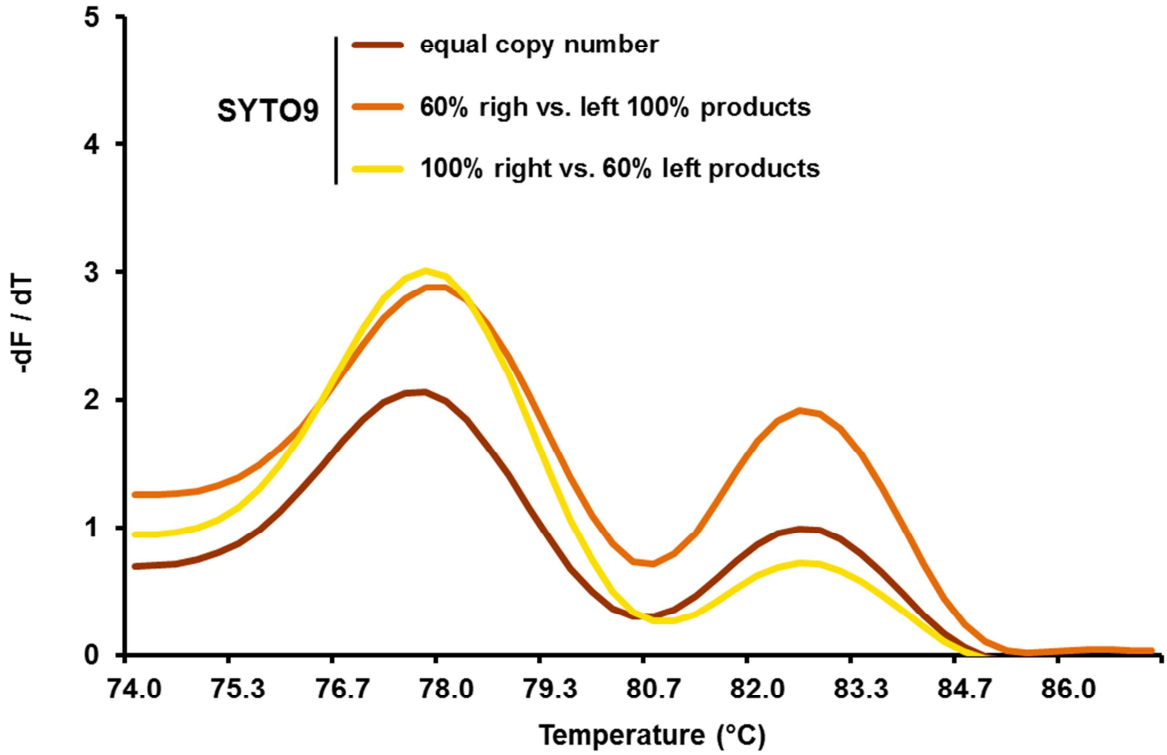

Figure 10. The recommended SYTO9 concentration is not sufficient to saturate two targets in a multiplexed MCA setup.

Employing 2 µM of the dye, additional SYTO9 molecules were able to interact with the unchanged product if either the AT- or the GC-rich amplicon was less abundant. Also, a high preference for AT-rich sequences was observed.

Note that the plot was not baseline corrected.

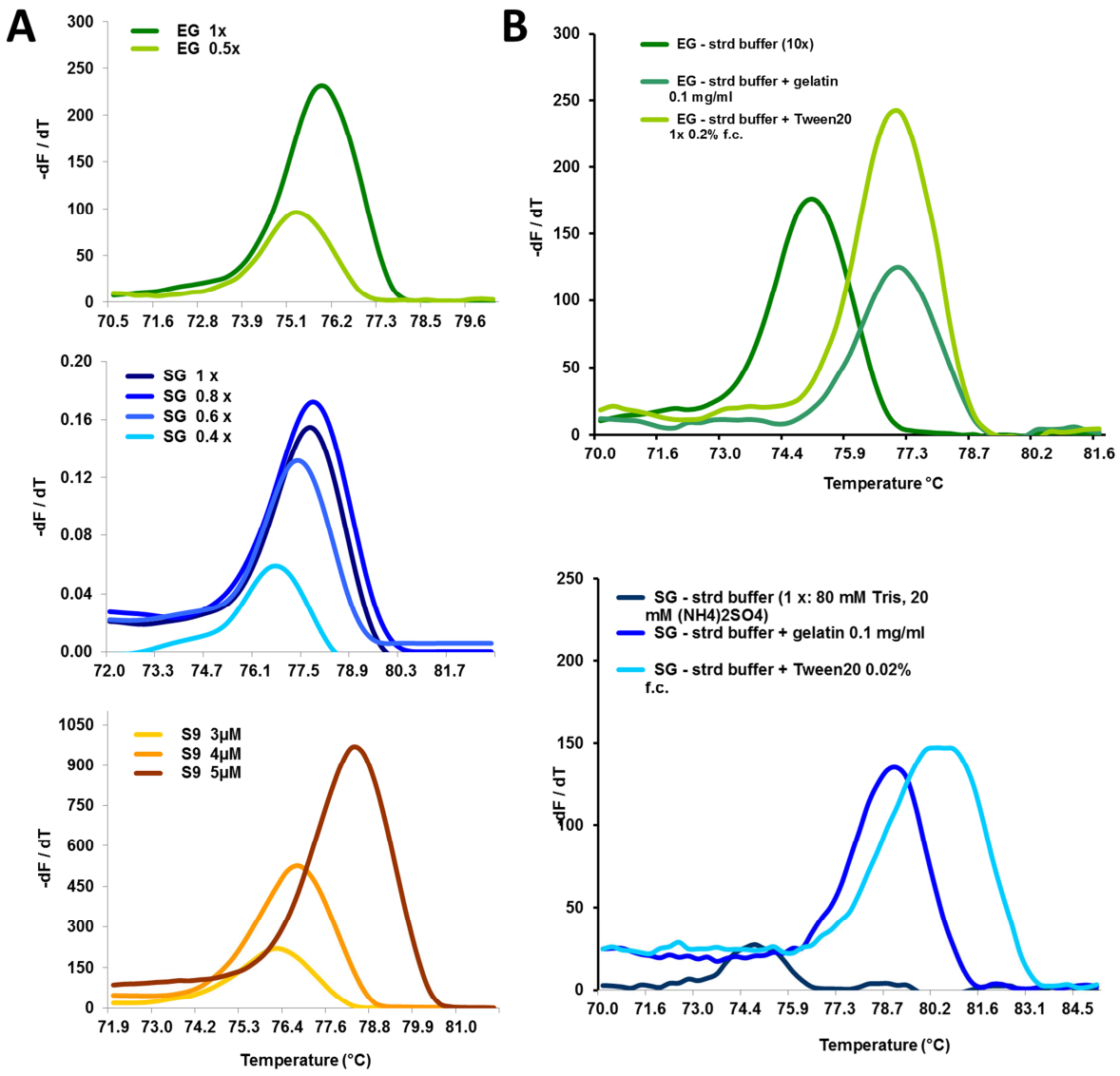

Figure 11. Dyes and different buffer components change the amplicon melting temperature.

A: Higher concentrations of the dyes SG and SYTO9 (S9) significantly increase the plotted Tm, while changes after enrichment with EG molecules are moderately.

B: Buffer components like the PCR enhancer chemicals gelatin and Tween20 significantly change the experimentally derived amplicon Tm compared to an enhancer free standard PCR buffer. They equally increase the fluorescence strength and the Tm. Whether the higher fluorescence level is due to reduced noise or higher dye molecule number per amplicon, was not evaluated for this work.

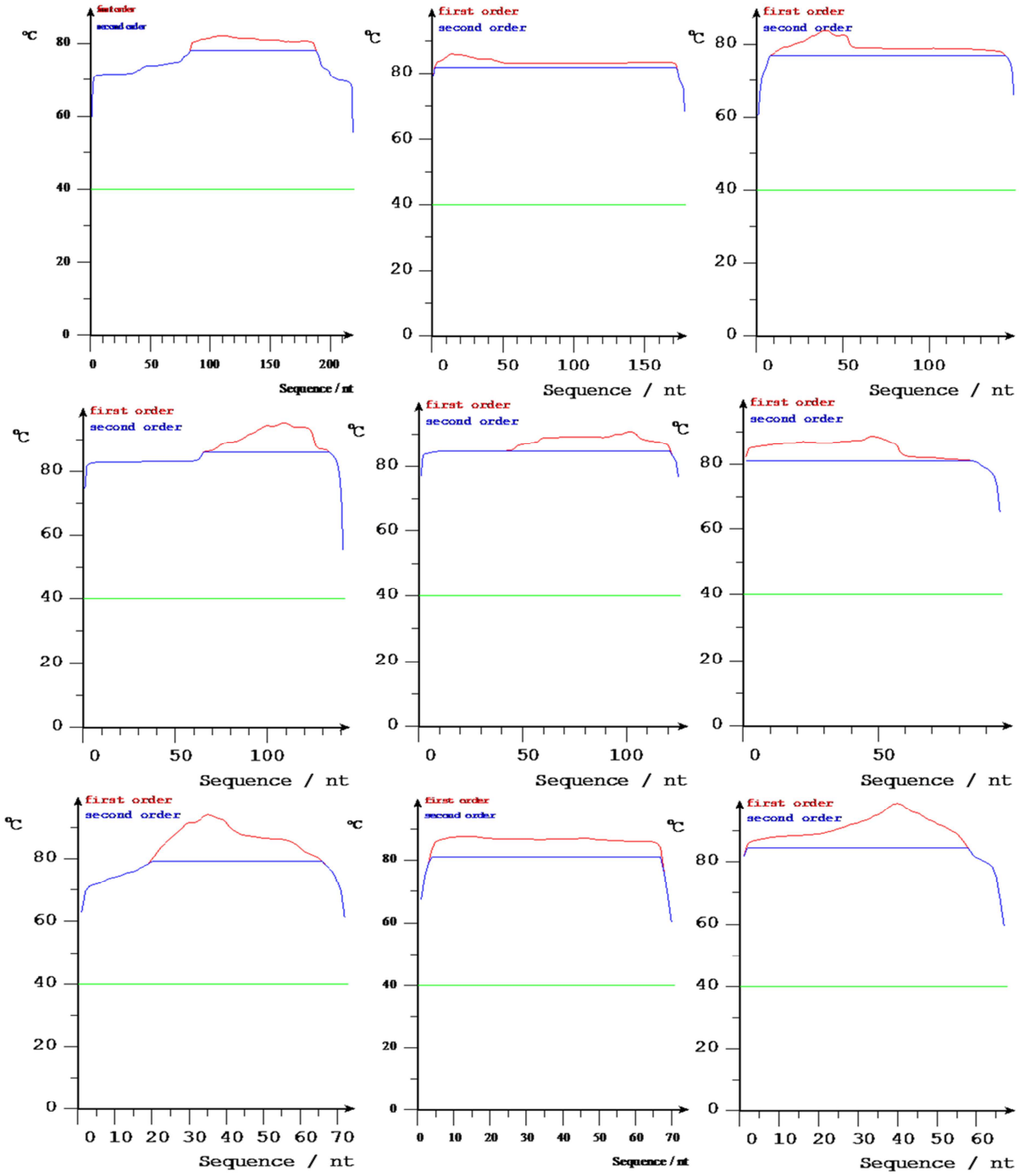

Figure 12. The online tool POLAND is useful to predict heat maps of different nucleotide sequences.

With the plotted calculation of the energetic background (Steger, 1994) it is possible to define extremely heat stable areas (red lines) or melting domains within the targeted sequence. The amplicon's Tm can be predicted using the second order trend line, since the matrix does not calculate a fixed value.

Note that the modifications found by Blake & Delcourt (1998) were additionally configured for all calculations.

Curriculum Vitae

Georg Mair

Education:

• 1986 – 1990 (summer)	VS 2 – Berta von Suttner Volksschule Linz/Biesenfeld
• 1990 – 1998 (summer)	Kollegium Petrinum Linz (humanistic college / AHS)
• A-levels (1998)	A-levels Kollegium Petrinum
• Since 1999	Diploma Study for the degree Mag.rer.nat., Microbiology and Genetics, University of Vienna

Positions held:

• **Permanent Jobs:**	Technician, VetCore, Genomics Core Facility, University for Veterinary Medicine Vienna (2007 – 2013) Technician, Laboratory for Tropical VetSciences, University of Veterinary Medicine Vienna (2013 – up to date)
• **Temporary Jobs:**	1. Lecturer and Guide for IAEA: Training Course for Molecular Methods – Botswana (2009)/Zambia (2011)/China (2012) 2. Laboratory Assistent: “Institute of cytological, histological and bacteriological Diagnostics” – Linz (one month)